

# Axial form factors of the octet baryons in a covariant quark model

G. Ramalho<sup>1</sup> and K. Tsushima<sup>1,2</sup>

<sup>1</sup>*International Institute of Physics, Federal University of Rio Grande do Norte, Campus Lagoa Nova - Anel Viário da UFRN, Lagoa Nova, Natal-RN, 59070-405, Brazil and*

<sup>2</sup>*Laboratório de Física Teórica e Computacional, LFTC, Universidade Cruzeiro do Sul, São Paulo 01506-000, Brazil*

(Dated: December 22, 2021)

We study the weak interaction axial form factors of the octet baryons, within the covariant spectator quark model, focusing on the dependence of four-momentum transfer squared,  $Q^2$ . In our model the axial form factors  $G_A(Q^2)$  (axial-vector form factor) and  $G_P(Q^2)$  (induced pseudoscalar form factor), are calculated based on the constituent quark axial form factors and the octet baryon wave functions. The quark axial current is parametrized by the two constituent quark form factors, the axial-vector form factor  $g_A^q(Q^2)$ , and the induced pseudoscalar form factor  $g_P^q(Q^2)$ . The baryon wave functions are composed of a dominant  $S$ -state and a  $P$ -state mixture for the relative angular momentum of the quarks. First, we study in detail the nucleon case. We assume that the quark axial-vector form factor  $g_A^q(Q^2)$  has the same function form as that of the quark electromagnetic isovector form factor. The remaining parameters of the model, the  $P$ -state mixture and the  $Q^2$ -dependence of  $g_P^q(Q^2)$ , are determined by a fit to the nucleon axial form factor data obtained by lattice QCD simulations with large pion masses. In this lattice QCD regime the meson cloud effects are small, and the physics associated with the valence quarks can be better calibrated. Once the valence quark model is calibrated, we extend the model to the physical regime, and use the low  $Q^2$  experimental data to estimate the meson cloud contributions for  $G_A(Q^2)$  and  $G_P(Q^2)$ . Using the calibrated quark axial form factors, and the generalization of the nucleon wave function for the other octet baryon members, we make predictions for all the possible weak interaction axial form factors  $G_A(Q^2)$  and  $G_P(Q^2)$  of the octet baryons. The results are compared with the corresponding experimental data for  $G_A(0)$ , and with the estimates of baryon-meson models based on  $SU(6)$  symmetry.

## I. INTRODUCTION

The electromagnetic and the weak structure of the hadrons can nowadays be accessed by electroweak probes, and characterized in terms of the corresponding structure form factors. There is presently a considerable information about the vector electroweak form factors, including the electromagnetic form factors of several baryons and mesons, where these form factors characterize the spatial distribution of the charge and magnetism [1]. As for the weak interaction axial form factors, from now on mentioned simply as axial form factors, the information is much more scarce. Only for the nucleon there are some data available for finite  $Q^2$ , where  $Q^2 = -q^2$  and  $q$  is the four-momentum transfer of the corresponding weak-axial transition. See Refs. [2–5] for a review of the nucleon axial form factors and Ref. [6] for the octet baryon axial form factors.

A better knowledge of the axial form factors of a baryon is very important, because it provides complementary information to the electromagnetic structure, and also because involves both the strong and weak interactions. The form factors associated with the weak interaction axial current for the transitions  $B' \rightarrow B \ell \bar{\nu}_\ell$ , with  $B, B'$  being spin 1/2 baryons,  $\ell = e, \mu, \tau$  and  $\bar{\nu}_\ell$  is a antineutrino, can be decomposed into the axial-vector

$G_A$  and induced pseudoscalar  $G_P$  form factors [6, 7]. In the limit  $Q^2 = 0$  the octet baryon form factors  $G_A$  can be related with the polarized deep inelastic scattering data, and used to estimate the spin fraction of the baryon carried by the quarks (valence and sea) [3, 8–13].

The nucleon axial-vector form factor can be accessed by (quasi)elastic (anti)neutrino scattering and by charged pion electroproduction experiments. The value for  $Q^2 = 0$  is determined accurately by the neutron  $\beta$  decay [2, 3, 5]. The induced pseudoscalar form factor can be determined at very low  $Q^2$  by pion production experiments and muon capture by a proton. In general the accuracy is worse compared with the electromagnetic form factors, and limited to the region  $Q^2 < 1 \text{ GeV}^2$  [2, 4]. A review of experimental data can be found in Refs. [2, 3, 5]. To improve our knowledge of the weak interaction axial structure of nucleon, more precise data for  $G_A$  are necessary for  $Q^2 < 1 \text{ GeV}^2$  as well as higher  $Q^2$ . In progress are several experiments for quasi-elastic (anti)neutrino scattering with proton targets (MINER $\nu$ A [14]) and nucleus targets (T2K [15] and ArgoNeuT [16]). Models for neutrino/antineutrino scattering based on baryon-meson coupled-channels can be found in Refs. [17–19].

The  $G_P$  data are very scarce, since they cannot be obtained by neutrino or antineutrino scattering [20]. The available data were obtained by pion electroproduction

and also by interaction with muons [2, 4]. The relevant data can be found in Refs. [21–23]. As for the axial-vector form factors of the octet baryons, the available information is limited to the values of  $G_A(0)$  for a few allowed transitions [6, 24].

The axial form factors of the octet baryons, including the nucleon, have been studied using constituent and chiral quark models [13, 25–37], based on the Dyson-Schwinger equations [38–41], models with meson cloud dressing [42–54], large- $N_C$  and chiral perturbation theory [5, 55–65] and QCD sum rules [66–68]. Recently, lattice QCD simulations for the nucleon became available for  $Q^2 = 0$  [69–76], for finite  $Q^2$  [77–83], and also for the octet baryons [84–87]. These studies are very important to understand the role of the valence quarks and of the meson cloud dressing. The role of the meson cloud dressing in the deep inelastic scattering, namely in the nucleon parton distribution functions, was studied in Refs. [88–91]. Of interest is also models based on the  $SU(3)$ -flavor symmetry of the baryon-meson reactions, like the heavy baryon  $SU(3)$  chiral perturbation theory, and others, which hereafter will simply be referred to as  $SU(3)$  baryon-meson models [6, 7, 56, 57]. Furthermore, modifications in the nuclear medium are also studied in Refs. [92–97].

In the present work we study the axial form factors of the nucleon and octet baryons using the covariant spectator quark model. The model has successfully been applied in studies of the electromagnetic structure of nucleon [98–100], several nucleon resonances [1, 101–105] and other baryons [106–114]. The covariant spectator quark model is based on the assumption that the constituent quarks have their own internal structure, which can be parametrized by individual quark (electromagnetic) form factors.

In this work we extend the formalism of the covariant spectator quark model for the weak interaction axial structure of baryons, by introducing the axial-vector  $g_A^q$  and induced pseudoscalar  $g_P^q$  form factors at the quark level.<sup>1</sup> Based on our construction of the quark axial current, we calculate the contribution of the valence quarks for the *macroscopic octet baryon* form factors  $G_A$  and  $G_P$ . The quark axial-vector form factor  $g_A^q$  can be defined *naturally* based on its isovector character, but  $g_P^q$  has to be calibrated through a vector meson dominance form by the lattice QCD data for the nucleon.

Once the model is calibrated by the lattice QCD data for the nucleon, we extrapolate the model from the lattice QCD regime to the physical regime, which allows to estimate the magnitude of the meson cloud contribution for the nucleon axial form factors.

In the present model the wave functions of the nucleon and the octet baryons are defined as in previous works [98, 106] using an  $S$ -state structure, but we include additionally a  $P$ -state component with an admixture coefficient  $n_P$ . The motivation to include the higher angular momentum states and the  $P$ -state is in particular comes from the Cloudy Bag Model (CBM) and nonrelativistic quark models [25, 27, 35, 39, 42]. The magnitude of the  $P$ -state component will be fixed by the comparison with the lattice QCD data for the nucleon with large pion masses, where the meson cloud contamination is very small.

After the calibration of the model by the nucleon data (lattice and physical), we extend the model parametrization to the octet baryons, and make predictions for the valence and valence plus meson cloud contributions for the form factors  $G_A$  and  $G_P$ . The results for the octet baryons are compared with the lattice QCD results as well as the  $SU(3)$  baryon-meson models.

To summarize, in this work we derive a successful parametrization for the nucleon axial form factors, valid both in the physical regime and lattice QCD regime. Finally, we make predictions for the octet baryon axial form factors.

This article is organized as follows. In Sec. II we introduce definitions of axial current and axial form factors, both for the nucleon and the octet baryons. In Sec. III we explain briefly the method used to calibrate the quark axial current and the  $P$ -state mixture in the nucleon wave function, based on the available data for the nucleon. The formalism of the covariant spectator quark model, including the definition of the quark axial current and the octet baryon wave functions, are presented in Sec. IV. In Secs. V and VI we present expressions obtained for the valence quark components for the axial form factors (bare or core form factors). In Sec. VII we explain how the effects of the meson cloud component can be taken into account for the physical regime. Predictions of the  $SU(3)$  baryon-meson model are discussed in Sec. VIII. Results for the nucleon and octet baryon axial form factors are presented respectively in Secs. IX and X. Finally, summary and conclusions are presented in Sec. XI.

## II. AXIAL-VECTOR AND INDUCED PSEUDOSCALAR FORM FACTORS

We define below the axial form factors of nucleon and their extensions for the other octet baryon members.

### A. Nucleon

The weak-axial transition between the nucleon states with an initial momentum  $P_-$  with a final momentum  $P_+$ , where  $q = P_+ - P_-$ , can be defined by the weak-

<sup>1</sup> We include the upper index  $q$  to emphasize that the functions are related with quarks, and also to avoid the confusion with the well established notation at the baryon level,  $g_A = G_A(0)$  and  $g_P = \frac{m_\mu}{2M} G_P(-0.88m_\mu^2)$ , where  $m_\mu$  is the muon mass.

axial current as [2–6]

$$(J_5^\mu)_a = \bar{u}(P_+) \left[ G_A(Q^2)\gamma^\mu + G_P(Q^2)\frac{q^\mu}{2M} \right] \gamma_5 u(P_-) \frac{\tau_a}{2}, \quad (2.1)$$

where  $M$  is the nucleon mass,  $\tau_a$  ( $a = 1, 2, 3$ ) are the isospin operators (Pauli matrices),  $u(P_\pm)$  the nucleon Dirac spinors, and  $G_A$  and  $G_P$  are respectively the axial-vector and induced pseudoscalar form factors. The "axial-tensor" form factor is ignored since it is associated with the second-class current and consistent with zero within experimental uncertainty [3–6]. The current  $(J_5^\mu)_a$  can be projected on the nucleon initial and final isospin states, using the isospin matrices, responsible for the  $SU(2)$ -flavor (isospin) symmetry [ $SU_F(2)$  space], acting on the isospin states of the nucleon.

The discussion of the form factors defined by Eq. (2.1) becomes simpler, when we use a spherical representation ( $a = 0, \pm$ ). Then we have neutral transitions when  $a = 0$  ( $n \rightarrow n$  and  $p \rightarrow p$ ) and the transitions  $n \leftrightarrow p$  for  $\tau_\pm$ . The weak neutral current ( $a = 0$ ), ( $\Delta I = 0$ ) corresponds to the  $Z$ -boson emission or absorption. The charged currents ( $a = \pm$ ) are associated with the  $\Delta I = \pm 1$  transitions mediated by the  $W$ -bosons emission or absorption for the  $p \leftrightarrow n$  transitions. In this work we simply assume that the function  $G_A(Q^2)$  is defined by the isovector transition form factor, that corresponds to the transition between the  $u$  and  $d$  quarks at the tree level.

Note that, experimentally the situation is more complex, and in practice there are corrections to the pure  $W$ - and  $Z$ -exchanges [3, 96]. From the theoretical point of view the important issues are, whether or not we can ignore the effects of the  $s$ -quark and sea quarks for the axial form factors of the nucleon  $G_A$  and  $G_P$  [2, 3].

Since the nucleon axial current is related with the quarks  $u$  and  $d$ , we can perform a flavor decomposition defining the isovector combination of the form factors [75, 81, 86]

$$G_A^{u-d} \equiv G_A^u - G_A^d. \quad (2.2)$$

The isoscalar combination can also be defined as

$$G_A^{u+d} \equiv G_A^u + G_A^d. \quad (2.3)$$

Note however, that the isoscalar axial-vector form factors cannot be obtained by a simple current operator, but they can be calculated in lattice QCD simulations using generalized form factors [80, 81].

If we assume charge symmetry using  $G_A^d = -\frac{1}{2}G_A^u$  according to the relation between the two quark charges, we obtain  $G_A^{u-d} = \frac{3}{2}G_A^u$  and  $G_A^{u+d} = \frac{1}{2}G_A^u$ . Equivalently  $G_A^{u-d} = 3G_A^{u+d}$ .

At  $Q^2 = 0$  the values of  $G_A^u(0) = \Delta\Sigma^u$  and  $G_A^d(0) = \Delta\Sigma^d$ , are related with the intrinsic spin of the valence quark  $q$  in the proton,  $\Delta\Sigma^q$ . These quantities are very

important for the estimate of the valence quark spin content of the proton [8–10, 13, 48, 81].

It is important to mention that in the lattice QCD simulations, contrarily to the isovector axial form factors, the isoscalar axial-vector form factor has contributions from the so-called disconnected diagrams, which are in general neglected in the simulations [75, 83]. The first calculation indicated that the disconnected diagrams can contribute about 10% for  $G_A$  and 20% for  $G_P$  [83]. In the present work we can ignore these corrections, since our axial current is identified with the isovector axial form factors.

The estimates of  $\Delta\Sigma^u$  and  $\Delta\Sigma^d$  based on deep inelastic scattering data, combined with the  $SU(3)$  symmetry are consistent with the charge symmetry ( $\Delta\Sigma^u/2 + \Delta\Sigma^d = -0.006 \pm 0.015$ ) [8]. The estimates from lattice QCD available at the moment are in agreement with the estimates based on deep inelastic scattering for  $\Delta\Sigma^u$ , but underestimates  $\Delta\Sigma^d$ , even when the disconnected contributions are taken into account [75, 83]. As a consequence, the results from lattice QCD violate charge symmetry ( $\Delta\Sigma^u/2 + \Delta\Sigma^d = 0.097 \pm 0.012$ ) [83]. It is worth to mention, however, that the lattice QCD calculations for the disconnected diagrams contributions are at the moment restricted to the pion masses around 370 MeV and the statistics is poor [75].

## B. Octet baryons

The axial form factors for the transition between the octet baryon members  $B$  and  $B'$  can be generalized taking into account the quark axial current  $\bar{u}\gamma^\mu\gamma_5 d$  ( $d \rightarrow u$ ) and  $\bar{u}\gamma^\mu\gamma_5 s$  ( $s \rightarrow u$ ) in the  $SU(3)$ -flavor quark model [ $SU_F(3)$  symmetry]. They are defined in terms of the weak-axial current as [55]

$$J_5^\mu = \frac{1}{2}\bar{u}_{B'}(P_+) \left[ G_A(Q^2)\gamma^\mu + G_P(Q^2)\frac{q^\mu}{2M_{BB'}} \right] \gamma_5 u_B(P_-), \quad (2.4)$$

where  $u_{B'}$  and  $u_B$  are the corresponding Dirac spinors, and  $M_{BB'}$  is the average mass of the final (mass  $M_{B'}$ ) and initial (mass  $M_B$ ) baryons:  $M_{BB'} = \frac{1}{2}(M_{B'} + M_B)$ . The factor 1/2 in Eq. (2.4) is included to be consistent with the nucleon case (2.1).

The form factors  $G_A(Q^2)$  and  $G_P(Q^2)$  defined by Eq. (2.1) are dependent on the octet baryon indices  $B$  and  $B'$ , similar to the nucleon case ( $p \rightarrow p$ ,  $n \rightarrow n$  and  $n \leftrightarrow p$ ). However, for simplicity we omit the baryon indices along the paper.

As in the case of the nucleon, weak transitions between the octet baryons can occur by the neutral current ( $Z$ -boson) and by the charged current ( $W^\pm$  boson). The neutral transitions, that do not change their charges or isospin states are  $N \rightarrow N$ ,  $\Sigma \rightarrow \Sigma$ ,  $\Xi \rightarrow \Xi$ ,  $\Sigma \rightarrow \Sigma$  and  $\Xi \rightarrow \Xi$ . The charged current transitions can be divided

in two kinds, the cases with  $\Delta I = 1$ , and the cases with  $\Delta S = 1$ . Here,  $\Delta I = 1$  and  $\Delta S = 1$  represent variations of  $\pm 1$  (variation of 1 in absolute value) of the isospin and strangeness, respectively. The transitions  $\Delta I = 1$  are associated with the  $u \leftrightarrow d$  transitions. Examples of those transitions are:  $n \rightarrow p$ ,  $\Sigma^+ \rightarrow \Lambda$ ,  $\Sigma^- \rightarrow \Lambda$ ,  $\Sigma^- \rightarrow \Sigma^0$  and  $\Xi^- \rightarrow \Xi^0$ . The transitions  $\Delta S = 1$  are associated with the  $u \leftrightarrow s$  transitions. In this case one has  $\Lambda \rightarrow p$ ,  $\Sigma^- \rightarrow n$ ,  $\Sigma^0 \rightarrow p$ ,  $\Xi^- \rightarrow \Lambda$ ,  $\Xi^- \rightarrow \Sigma^0$  and  $\Xi^0 \rightarrow \Sigma^+$ .

It is important to note that the form factors associated with the  $\Delta I = 1$  and  $\Delta S = 1$  transitions contribute differently for the transition cross sections [6]. The  $\Delta I = 1$  form factors are multiplied by the factor  $\cos \theta_C \simeq 0.97$ , while the  $\Delta S = 1$  form factors are multiplied by the factor  $\sin \theta_C \simeq 0.23$ . In the neutral current transitions the factor is 1.

The transition current between the octet baryon members can also be represented by an  $SU_F(3)$  extension of  $SU_F(2)$  using the Gell-Mann matrices  $\lambda_a$  ( $a = 1, \dots, 8$ ) instead of the Pauli matrices  $\tau_a$  ( $a = 1, 2, 3$ ) [115]. In this case the transition currents are expressed in terms of the octet baryon states, or by the  $3 \times 3$  baryon matrix and flavor-transition operators in the corresponding octet vector space [7, 57, 59, 116].

### III. METHODOLOGY

We discuss now the method used to calculate the axial form factors of the nucleon and the other members of octet baryons within the framework of the covariant spectator quark model. We start by the nucleon case. Later, we extend the framework for the other octet baryons. The formalism of the covariant spectator quark model is reviewed briefly in the next section.

In the covariant spectator quark model the electromagnetic structure of the baryons is described based on the valence quark structure of the baryon wave functions, and the electromagnetic structure of the constituent quarks. The electromagnetic structure of the baryons is parametrized by the quark electromagnetic form factors which simulate effectively the internal structure of the constituent quarks resulting from the interactions with quark-antiquark pairs and from the gluon dressing [98, 107]. Of particular relevance for the present work is the quark isovector form factors  $f_{1-}$  and  $f_{2-}$ , associated respectively with the Dirac and Pauli components of the constituent quark current [see the following Sec. IV A for the details]. In the present study we define two new quark form factors,  $g_A^q$  and  $g_P^q$ , respectively the quark axial-vector and quark induced pseudoscalar form factors. The details are discussed in Sec. IV B.

In order to calculate the axial form factors of the nucleon, we need a model for the wave function of the nucleon. We start assuming that we can describe the nucleon as a quark-diquark system with an  $S$ -state configuration following Ref. [98]. Previous works had shown

that an  $S$ -state quark-diquark system is a good approximation for the nucleon [117–119].

Since the structure based only on an  $S$ -state is quite poor as we will show in Sec. V, we consider a possibility of adding a  $P$ -state mixture to the nucleon wave function. The motivation to include this new component comes from nonrelativistic quark models, QCD sum rules, and also from CBM [39, 42, 67]. In some models the  $P$ -state mixture corresponds to the lower component of the nucleon Dirac spinor, which becomes very important for the axial form factors in a relativistic treatment [27, 39, 42]. In the covariant spectator quark model the  $P$ -state quark-diquark wave function is generated by the integration on the quark-pair internal degrees of freedom in the three-quark wave function. The quark-diquark wave function contains all the information originally included in the three-quark wave function, as discussed in Ref. [99]. This  $P$ -state quark-diquark wave function appears as the consequence of the relativity and vanishes in the nonrelativistic limit [99].

We consider then a nucleon wave function composed of a combination of the  $S$ - and  $P$ -state components, parametrized by the  $P$ -state mixing coefficient  $n_P$  ( $n_P^2$  gives the  $P$ -state probability in the nucleon wave function). The coefficient of the  $S$ -state,  $n_S$ , is expressed by  $n_S = \sqrt{1 - n_P^2}$ . When  $n_P = 0$  ( $n_S = 1$ ), we recover the  $S$ -state wave function.

The discussion about how the  $P$ -state can be built within the covariant spectator quark model is presented in Ref. [99]. The radial wave function associated with the  $S$ -state was already determined by the study of the electromagnetic structure of nucleon. For the  $P$ -state component, the corresponding radial wave function can be defined in terms of the radial wave function of the  $S$ -state, without introducing any extra parameter [9, 98].

As a consequence of the underlying internal structure of the nucleon based on the valence quark degrees of freedom, we decompose the nucleon axial form factors, admitting the possibility of meson excitations of the core, as

$$G_A(Q^2) = G_A^B(Q^2) + G_A^{MC}(Q^2), \quad (3.1)$$

$$G_P(Q^2) = G_P^{\text{pole}}(Q^2) + G_P^B(Q^2) + G_P^{MC}(Q^2), \quad (3.2)$$

where  $G_A^B$  and  $G_P^B$  are the contributions from the bare core (valence quark contribution), while  $G_A^{MC}$  and  $G_P^{MC}$  are those from the meson cloud. The meson pole term  $G_P^{\text{pole}}$  is an additional contribution that is the result of a meson creation by the baryon transition that decays by the weak interaction, into a lepton-neutrino pair [2, 4, 5, 55].

For the nucleon and other non-strangeness changing transitions ( $\Delta I = 1$ ), the pion (mass  $m_\pi$ ) is expected to give a dominant contribution in the meson pole contributions, which is determined by the partial conservation of the axial current (PCAC) [2, 4, 5, 42, 43, 55, 78]

$$G_P^{\text{pole}}(Q^2) = \frac{4M^2}{m_\pi^2 + Q^2} G_A^B(Q^2). \quad (3.3)$$



In the study of the  $Q^2$ -dependence of the form factors  $G_P$ , the pole term is very important, especially in the timelike region ( $Q^2 < 0$ ) [2]. Note that, contrarily to most of the works in literature, in r.h.s. of Eq. (3.3), we use  $G_A^B(Q^2)$  the bare contribution, instead of the function  $G_A(Q^2)$ , the total result for the axial-vector form factor, which includes also the meson cloud contribution. We replace  $G_A$  by  $G_A^B$  because we want to use the relation (3.3) also in the lattice QCD regime, in the limit where the meson cloud effects are small. In the cases where meson cloud effects are significant for  $G_A$ , as in the physical limit, the term  $\frac{4M^2}{m_\pi^2+Q^2}G_A^{MC}$  can be interpreted as a meson cloud contribution for  $G_P$ . In the literature  $G_A$  is often replaced by parametrizations of the experimental data labeled here as  $G_A^{\text{exp}}(Q^2)$  [2, 22].

The factor  $G_P^{\text{pole}}$  can be connected with the strong pion-nucleon coupling at  $Q^2 = 0$  in the chiral limit, via the Goldberger-Treiman relation [120]. For a more complete discussion see Refs. [2, 4, 5, 42, 43].

Note that, since we have contribution from the valence quark core for  $G_P$ , we are including at  $Q^2 = 0$  corrections to the Goldberger-Treiman relation according to (3.2). This is not a problem, since the relation is strictly valid only in the chiral limit, and some corrections are expected, according to chiral perturbation theory and other frameworks [2, 4, 35, 38, 43, 55]. Calculations of  $G_P$  can be found in Refs. [30, 31, 34, 38, 43, 44, 61, 67, 68]. For a review about the theory and experimental data associated with  $G_P$ , see Ref. [4].

In the limit where the meson cloud effects are small, we can drop the meson cloud contributions  $G_A^{MC}$  and  $G_P^{MC}$  and consider only the contributions from the bare core, and the pole term in the case of  $G_P$ . This situation occurs when we deal with lattice QCD simulations with large pion masses (large  $m_\pi$ ). Along this work we will use the expression “the large pion masses” to indicate the range  $m_\pi > 350$  MeV.

If the covariant spectator quark model is successful in the description of the bare core contribution of the nucleon axial form factors, it should also be able to reproduce the lattice QCD data for large  $m_\pi$ , since in the lattice QCD regime the model is dominated by the valence quark effects. Therefore in this work, we use the lattice QCD data with large  $m_\pi$  to calibrate the valence quark contributions of the model for the axial form factors. At the end the model will be extrapolated to the physical regime ( $m_\pi = m_\pi^{\text{phys}} \simeq 138$  MeV) and will be used to estimate the contributions of the meson cloud to the nucleon form factors.

An important step is the extension of the covariant spectator quark model to the lattice QCD regime. This will be done taking advantage of our parametrization for the quark form factors, both electromagnetic and axial currents, which are defined based on vector meson dominance (VMD) parametrizations. The extension of the model to the lattice QCD regime will be discussed in Sec. IV E.

A model based exclusively on the valence quark degrees

of freedom is particularly convenient to compare with the lattice QCD data with large  $m_\pi$ . In this case we have a more clean parametrization (free of meson cloud effects) for the valence quark effects. The same method was used previously and successfully in the studies of the electromagnetic properties of the nucleon, the Roper, the  $\gamma^*N \rightarrow \Delta$  reaction, as well as in the studies of the octet and decuplet baryon properties [102–104, 106–109].

The methodology used in the present study can be summarized as follows:

- First, we calibrate our model by a fit to the lattice QCD data for  $G_A(Q^2)$ . The calculation of  $G_A(Q^2)$  depends on the quark axial-vector form factor  $g_A^q(Q^2)$  and the amount of the  $P$ -state mixture ( $n_P$ ). Since  $g_A^q(Q^2)$  is associated with an isovector structure we simply assume that the  $Q^2$  dependence of  $g_A^q(Q^2)$  can be approximated by the quark Dirac isovector form factor  $f_{1-}$ . Under this assumption we try to find if there are proper values for  $n_P$  that can describe the nucleon lattice QCD data for  $G_A$ . We conclude that the answer is positive, and  $n_P$  is determined by the best fit to the data. Up to this stage we neglect the induced pseudoscalar form factor of the quark by setting  $g_P^q \equiv 0$ .
- Next, we check whether or not the lattice data for  $G_P(Q^2)$ , associated with several values of  $m_\pi$ , can be described by a simple model for the quark induced pseudoscalar form factor  $g_P(Q^2)$ , parametrized by a VMD form. Again, the answer turns out to be positive, and we use the lattice QCD data to estimate the shape of  $g_P^q$ , fixing the two parameters of the VMD expression. With the determination of  $n_P$  and  $g_P^q(Q^2)$  by the fit to the lattice data, we finish the calibration of the valence quark component of our model.
- The next step is to extrapolate the model to the physical regime ( $m_\pi \rightarrow m_\pi^{\text{phys}}$ ). The extrapolation is performed in two steps. First, we extrapolate our parametrization of the valence quark contributions (obtained from the lattice QCD data) to the physical regime, to get  $G_A^B(Q^2)$  and  $G_P^B(Q^2)$ . Next, we correct the result for the form factors including the normalization factor of the wave function,  $\sqrt{Z_N}$ , corresponding to the fraction of the three-quark valence quark system, in the physical nucleon wave function, redefining the effective contribution of the valence quarks by effectively taking into account the meson cloud effects. With this procedure  $G_A^B$  is modified according to

$$G_A^B(Q^2) \rightarrow Z_N G_A^B(Q^2). \quad (3.4)$$

We estimate  $Z_N$  by comparing our valence quark model result with a parametrization extracted from the physical data  $G_A^{\text{exp}}(Q^2)$  in the region  $Q^2 \gtrsim 1$  GeV<sup>2</sup>, where the meson cloud effects are expected to be small. With this procedure we determine a

parametrization for the valence quark contribution, for the nucleon axial-vector form factor in the physical regime. After this the meson cloud effects can be estimated using  $G_A^{\text{exp}}(Q^2) - Z_N G_A^B(Q^2)$ . Also for the induced pseudoscalar form factor  $G_P$ , the contribution of the valence quarks  $G_P^B$  is corrected by the factor  $Z_N$ , in the physical limit. Details of the procedure are discussed in Sec. VII.

- With the model calibrated for the nucleon axial form factors ( $n \rightarrow p$  transition), we use  $SU_F(3)$  symmetry at the quark level to extrapolate the results of the nucleon to make predictions for the other octet baryon axial form factors. In Sec. VI we discuss our extrapolation from  $SU_F(2)$  to  $SU_F(3)$ . To obtain the final result for the octet baryon axial form factors, we need also to take into account the meson cloud effects for the other octet baryon members, which can be done making some assumptions about the amount of the meson cloud contribution based on  $SU(3)$  and/or  $SU(6)$  symmetries. Finally, we compare the results with those of the  $SU(6)$  baryon-meson model discussed in Sec. VIII.

#### IV. COVARIANT SPECTATOR QUARK MODEL

We discuss now the covariant spectator quark model. The covariant spectator quark model was first developed for the study of the electromagnetic properties of nucleon [98–100], and subsequently extended for the studies of the electromagnetic properties of several resonances, and electromagnetic transitions between baryon states [105, 113, 114], including the octet and decuplet baryons [106, 107, 109–112].

In the following, we review the formalism of the covariant spectator quark model related with the electromagnetic structure of the quarks and baryons. Next, we introduce the quark axial form factors, and explain how the axial current between the baryon states is calculated. Later, we describe the structure of the nucleon wave function in term of the valence quark structure, and explain how it can be extended for the octet baryons. Finally, we show how the model can be generalized to the lattice QCD regime.

##### A. Electromagnetic form factors

In the covariant spectator quark model the electromagnetic transition current is calculated in a relativistic impulse approximation using the nucleon wave function  $\Psi_N$  expressed in terms of the states of the quark 3 and the quark current  $j_q^\mu$  [98, 99, 107]:

$$J^\mu = 3 \sum_{\Gamma} \int_k \bar{\Psi}_N(P_+, k) j_q^\mu \Psi_N(P_-, k). \quad (4.1)$$

In the above the integral symbol represents the covariant integration associated with the diquark three-momentum,  $\Gamma$  represents the diquark polarizations (scalar and axial-vector), and  $k$  the diquark momentum. As before  $P_+$  and  $P_-$  are respectively the final and initial nucleon momenta.

The quark electromagnetic form factors are defined by the quark electromagnetic current  $j_q^\mu$  as [98, 101]:

$$j_q^\mu = \left( \frac{1}{6} f_{1+} + \frac{1}{2} f_{1-\tau_3} \right) \gamma^\mu + \left( \frac{1}{6} f_{2+} + \frac{1}{2} f_{2-\tau_3} \right) \frac{i\sigma^{\mu\nu} q_\nu}{2M}. \quad (4.2)$$

The functions  $f_{1\pm}$  define the Dirac isoscalar/isovector form factor and  $f_{2\pm}$  define the Pauli isoscalar/isovector form factor.

For the present discussion it is sufficient to mention the isovector form factors,  $f_{1-}$  and  $f_{2-}$ . These form factors were defined in previous works using a parametrization motivated by vector meson dominance [98, 101]:

$$f_{1-} = \lambda + (1 - \lambda) \frac{m_\rho^2}{m_\rho^2 + Q^2} + c_- \frac{Q^2 M_h^2}{(M_h^2 + Q^2)^2}, \quad (4.3)$$

$$f_{2-} = \kappa_- \left\{ d_- \frac{m_\rho^2}{m_\rho^2 + Q^2} + (1 - d_-) \frac{M_h^2}{M_h^2 + Q^2} \right\}, \quad (4.4)$$

where  $m_\rho$  is the  $\rho$  meson mass and  $M_h$  represents a mass of an effective heavy meson that simulates the structure of all the high mass resonances. The parameters  $\lambda$ ,  $\kappa_-$ ,  $c_-$  and  $d_-$  are coefficients calibrated by the nucleon form factor data and deep inelastic scattering (for  $\lambda$ ) [98]. We choose in particular the model II in Ref. [98], where  $\lambda = 1.21$ ,  $\kappa_- = 1.823$ ,  $c_- = 1.16$  and  $d_- = -0.686$ . As for  $M_h$  we use  $M_h = 2M$  (twice the nucleon mass) in order to simulate the short range structure of the current.

##### B. Axial form factors

Similarly to the electromagnetic form factors, the nucleon axial current can be written as

$$J_5^\mu = 3 \sum_{\Gamma} \int_k \bar{\Psi}_N(P_+, k) (j_{Aq}^\mu) \Psi_N(P_-, k). \quad (4.5)$$

The constituent quark axial current,  $j_{Aq}^\mu$  is defined in terms of the quark axial form factors  $g_A(Q^2)$  and  $g_P(Q^2)$  as

$$j_{Aq}^\mu = \left( g_A^q \gamma^\mu + g_P^q \frac{q^\mu}{2M} \right) \gamma_5 \frac{\tau_a}{2}. \quad (4.6)$$

As for the nucleon, we can add an isospin label  $a$  to the quark form factors  $g_A^q$  and  $g_P^q$ , but only one function is relevant due to the isospin symmetry. The form factor  $g_A^q$  is associated with the  $u \leftrightarrow d$  quark transitions ( $W$ -boson emission or absorption) responsible by the  $\Delta I = 1$  transitions.

As for  $g_A^q$ , we assume that it is the same as the isovector component of the Dirac form factor defined by Eq. (4.2), due to its isovector character:

$$g_A^q(Q^2) \equiv f_{1-}(Q^2). \quad (4.7)$$

Note that, then  $g_A^q(0) = 1$  [42, 121].

As for  $g_P^q$  we may be tempted to relate it with  $f_{2-}$ , because we expect a falloff,  $g_P^q \propto 1/Q^2$ . However, since the structure of the Pauli term and the term associated with the induced pseudoscalar current are very different, we choose instead only a form inspired by  $f_{2-}$ , given by

$$g_P^q(Q^2) = \alpha \frac{m_\rho^2}{m_\rho^2 + Q^2} + \beta \frac{M_h^2}{M_h^2 + Q^2}, \quad (4.8)$$

where the coefficients  $\alpha$  and  $\beta$  will be determined by a fit to the lattice QCD data obtained with large  $m_\pi$  (small meson cloud contamination).

To summarize, we choose parametrizations for the quark axial form factors  $g_A^q$  and  $g_P^q$ , motivated by VMD, similarly to what was done previously for the quark electromagnetic form factors,  $f_{i\pm}$  ( $i = 1, 2$ ).

### C. Nucleon wave function

For the nucleon wave function, we consider a mixture of the  $S$ - and  $P$ -states as suggested by Ref. [99],

$$\Psi_N(P, k) = n_S \Psi_S(P, k) + n_P \Psi_P(P, k), \quad (4.9)$$

where  $n_P$  is the  $P$ -state mixture coefficient, and  $n_S = \sqrt{1 - n_P^2}$ , as discussed already.

For the  $S$ -state  $\Psi_S(P, k)$ , we use [98]

$$\Psi_S(P, k) = \frac{1}{\sqrt{2}} [\phi^0 u(P) - \phi^1 (\varepsilon_P^*)_\alpha U^\alpha(P)] \psi_S(P, k), \quad (4.10)$$

where  $\phi^{0,1}$  are the isospin wave functions,  $\varepsilon_P^\alpha$  is the diquark polarization vector,  $U^\alpha(P)$  a spin 1/2 state, to be defined next, and  $\psi_S$  is the radial wave function.

The isospin wave functions,  $\phi^{0,1}$ , can be represented in terms of the isospin-0 and isospin-1 components that are also function of the nucleon isospin projection  $I_z$ , that labels the proton ( $I_z = +\frac{1}{2}$ ) and the neutron ( $I_z = -\frac{1}{2}$ ) states. More specifically, we can write [98]

$$\phi^0(I_z) = \xi^{0*} \chi(I_z), \quad (4.11)$$

$$\phi^1(I_z) = -\frac{1}{\sqrt{3}} (\tau \cdot \xi^{1*}) \chi(I_z), \quad (4.12)$$

where  $\chi(I_z)$  are the nucleon isospin state, that correspond also the isospin state of the quark-3 ( $u$  or  $d$ ), and  $\tau_\pm = \tau_x \pm i\tau_y$ , are the isospin raising and lowering operators and  $\tau_0 = \tau_z$ . The operators  $\xi^{0,1}$  are represented

as [98]

$$\xi^0 = \frac{1}{\sqrt{2}} (ud - du), \quad (4.13)$$

$$\xi_0^1 = \frac{1}{\sqrt{2}} (ud + du) = \xi_z, \quad (4.14)$$

$$\xi_+^1 = uu = -\frac{1}{\sqrt{2}} (\xi_x + i\xi_y), \quad (4.15)$$

$$\xi_-^1 = dd = \frac{1}{\sqrt{2}} (\xi_x - i\xi_y). \quad (4.16)$$

In the next section, we use an alternative notation to represent the flavor states of the remaining octet baryon members.

The spin-1 diquark component of the wave function (4.10) includes the spin state [101]

$$U^\alpha(P) = \frac{1}{\sqrt{3}} \gamma_5 \left( \gamma^\alpha - \frac{P^\alpha}{M} \right) u(P). \quad (4.17)$$

The spin states are ruled by the  $SU(2)$ -spin symmetry [ $SU_S(2)$  symmetry]. The spin 1/2 states  $U^\alpha(P)$  is combined with the diquark polarization vector,  $\varepsilon_P^\alpha(\lambda)$  ( $\lambda = 0, \pm$ ) defined in a fixed-axis base, for a three-momentum  $\mathbf{P}$  along the  $z$ -axis [100],

$$\varepsilon_P^\alpha(\pm) = \mp \frac{1}{\sqrt{2}} (0, 1, \pm 1, 0), \quad (4.18)$$

$$\varepsilon_P^\alpha(0) = \frac{1}{M} (P, 0, 0, E), \quad (4.19)$$

where  $E = \sqrt{M^2 + \mathbf{P}^2}$ .

In order to write the expression for the  $P$ -state conveniently, we define

$$\tilde{k} = k - \frac{P \cdot k}{M^2} P. \quad (4.20)$$

Note that at the nucleon rest frame,  $P = (M, 0, 0, 0)$ ,  $\tilde{k} = (0, \mathbf{k})$  is reduced to the diquark three-momentum, and  $\tilde{k}^2 = -\mathbf{k}^2$ . Following Ref. [99] we define the  $P$ -state wave function as

$$\Psi_P(P, k) = \frac{1}{\sqrt{2}} \tilde{k} [\phi^0 u(P) - \phi^1 (\varepsilon_P^*)_\alpha U^\alpha(P)] \psi_P(P, k), \quad (4.21)$$

where  $\psi_P(P, k)$  is the  $P$ -state radial wave function. Since the wave function (4.21) is reduced to two *upper* components that vanishes in the nucleon rest frame, the state correspond to a positive parity state (the negative parity of the  $P$ -state is cancelled by the negative sign from the Dirac parity operator  $\gamma^0$ ) [99].

The normalization conditions of the  $S$ - and  $P$ -state components require that,

$$\int_k [\psi_S(\bar{P}, k)]^2 = 1, \quad (4.22)$$

$$\int_k (-\tilde{k}^2) [\psi_P(\bar{P}, k)]^2 = 1, \quad (4.23)$$

where  $\vec{P} = (M, 0, 0, 0)$  is the nucleon momentum in its rest frame. The above conditions, derived from the  $Q^2 = 0$  limit, ensures that the charge of the nucleon state is  $e_N = \frac{1}{2}(1 + \tau_3)$ . [The operator  $e_N$  acts on the isospin states of the nucleon.]

The radial wave function for the  $S$ -state,  $\psi_S(P, k)$ , can be defined in terms of the dimensionless variable [98, 107]

$$\chi = \frac{(M - m_D)^2 - (P - k)^2}{Mm_D}. \quad (4.24)$$

As in previous works, we consider the form [98, 106],

$$\psi_S(P, k) = \frac{N_S}{m_D(\beta_1 + \chi)(\beta_2 + \chi)}, \quad (4.25)$$

where  $N_S$  is a normalization constant, and  $\beta_1, \beta_2$  are momentum scale parameters in units of  $Mm_D$ . In the present work we use the values  $\beta_1 = 0.049$  and  $\beta_2 = 0.717$  [98].

As for the  $P$ -state, we define  $\psi_P(P, k)$  as

$$\psi_P(P, k) = \frac{\psi_S(P, k)}{\sqrt{-\tilde{k}^2}}. \quad (4.26)$$

In this case both the  $S$ - and  $P$ -state components of the nucleon wave function are defined by the  $S$ -state parametrization established in previous works [98, 101].

#### D. Extension of the valence quark model for the octet baryons

We discuss now the extension of the model for the other members of the octet baryons. For this we need to consider the modifications of the quark axial current (4.6) as well as the modifications in the wave functions of the baryons.

We can extend the description of the nucleon wave function for the  $S$ - and  $P$ -states given by Eqs. (4.10) and (4.21), to the octet baryons replacing the isospin wave functions of the nucleon  $\phi^0$  and  $\phi^1$  by the mixed anti-symmetric and mixed symmetric  $SU(3)$  flavor wave functions, respectively  $|M_A\rangle_B$  and  $|M_S\rangle_B$  associated with the baryon  $B$ . The flavor wave functions,  $|M_A\rangle_B$ ,  $|M_S\rangle_B$  are presented in Table I.

As for the radial wave functions we follow the study of the electromagnetic properties of the octet baryons  $\Lambda$ ,  $\Sigma$  and  $\Xi$  based on the  $S$ -state [109]

$$\psi_{\Lambda,S}(P, k) = \frac{N_\Lambda}{m_D(\beta_1 + \chi_\Lambda)(\beta_3 + \chi_\Lambda)}, \quad (4.27)$$

$$\psi_{\Sigma,S}(P, k) = \frac{N_\Sigma}{m_D(\beta_1 + \chi_\Sigma)(\beta_3 + \chi_\Sigma)}, \quad (4.28)$$

$$\psi_{\Xi,S}(P, k) = \frac{N_\Xi}{m_D(\beta_1 + \chi_\Xi)(\beta_4 + \chi_\Xi)}, \quad (4.29)$$

where  $\chi_B$  is defined by Eq. (4.24) with  $M$  replaced by  $M_B$ ,  $N_B$  are normalization constants, and  $\beta_3, \beta_4$  are new

momentum range parameters (in units of  $M_B m_D$ ). The motivation for the above expressions is to modulate the short range behavior  $\beta_2$ , defined in the nucleon radial wave function by a different parameter (smaller value for  $\beta_3$  and  $\beta_4$ ) according to the number of strange quarks. We take the values from Ref. [109]:  $\beta_3 = 0.603$  and  $\beta_4 = 0.381$ . Similarly to the nucleon, we can also define the  $P$ -state radial wave functions as  $\psi_{B,P} = \psi_{B,S}/\sqrt{-\tilde{k}^2}$ , where  $\tilde{k}$  is defined by Eq. (4.20) in terms of the baryon momentum  $P$ .

The quark axial current (4.6) defined so far in the  $SU_F(2)$  sector, is extended to the  $SU_F(3)$  sector for transitions between the other octet baryons replacing the Pauli matrices  $\tau_a$  ( $a = 1, 2, 3$ ) by the Gell-Mann matrices  $\lambda_a$  ( $a = 1, \dots, 8$ ).

Using the Gell-Mann matrices we can describe the neutral current transitions ( $B \rightarrow B$ ) when the operator is  $I_0 = \lambda_3$ , and also the transitions with  $\Delta I = 1$  or  $\Delta S = 1$ . The transitions with  $\Delta I = 1$  are associated with the operator  $I_\pm = \frac{1}{2}(\lambda_1 \pm i\lambda_2)$  which correspond to the  $d \rightarrow u$  ( $I_+$ ) and  $u \rightarrow d$  ( $I_-$ ) transitions. The transitions with  $\Delta S = 1$  are associated with the operator  $V_\pm = \frac{1}{2}(\lambda_4 \pm i\lambda_5)$  which correspond to the  $s \rightarrow u$  ( $V_+$ ) and  $u \rightarrow s$  ( $V_-$ ) transitions.

According to the  $SU_F(3)$  symmetry the quark form factors  $g_A^q$  and  $g_P^q$  are the same as in the  $SU_F(2)$  sector. Therefore, once the model is fixed in the  $SU_F(2)$  sector, the results for the  $SU_F(3)$  sector represent predictions of the model.

#### E. Lattice QCD regime

We discuss here how we can perform the extension of the covariant spectator quark model to the lattice QCD regime. This extension was already done in the past for electromagnetic transitions [102, 103, 106, 109].

In the previous sections we have shown that the wave functions of the baryons, including the radial part  $\psi_S$  and  $\psi_P$ , can be written in terms of the baryon mass  $M_B$ . In Eq. (4.24) we have presented the parametrization for the nucleon, but the generalization for other baryons can be done by replacing  $M$  by the corresponding baryon mass  $M_B$ . We have also discussed how the quark axial current  $j_{Aq}^\mu$  given by Eq. (4.6) can be defined in terms of the axial form factors  $g_A^q$  and  $g_P^q$ , and the nucleon mass  $M$ . We have also concluded that the quark axial form factors can be represented by a VMD parametrization in terms of the mass of the vector meson mass ( $\rho$  meson), and an effective heavy meson with mass  $M_h = 2M$ .

Since the bare contribution for the electromagnetic and the axial form factors can be completely determined by the masses of the baryon ( $M_B$ ), the  $\rho$  mass ( $m_\rho$ ) and the nucleon mass ( $M$ ), we extend the model for the lattice QCD regime replacing these masses by the corresponding masses in the lattice QCD simulations. The remaining parameters in the quark current and in radial wave functions are the same as those used in the physical limit.



$B$	$ M_A\rangle$	$ M_S\rangle$
$p$	$\frac{1}{\sqrt{2}}(ud - du)u$	$\frac{1}{\sqrt{6}}[(ud + du)u - 2uud]$
$n$	$\frac{1}{\sqrt{2}}(ud - du)d$	$-\frac{1}{\sqrt{6}}[(ud + du)d - 2ddu]$
$\Lambda^0$	$\frac{1}{\sqrt{12}}[s(du - ud) - (dsu - usd) + 2(ud - du)s]$	$\frac{1}{2}[(dsu - usd) - s(ud - du)]$
$\Sigma^+$	$\frac{1}{\sqrt{2}}(us - su)u$	$\frac{1}{\sqrt{6}}[(us + su)u - 2uus]$
$\Sigma^0$	$\frac{1}{2}[(dsu + usd) - s(ud + du)]$	$\frac{1}{\sqrt{12}}[s(ud + du) + (dsu + usd) - 2(ud + du)s]$
$\Sigma^-$	$\frac{1}{\sqrt{2}}(ds - sd)d$	$\frac{1}{\sqrt{6}}[(sd + ds)d - 2dds]$
$\Xi^0$	$\frac{1}{\sqrt{2}}(us - su)s$	$-\frac{1}{\sqrt{6}}[(us + su)s - 2ssu]$
$\Xi^-$	$\frac{1}{\sqrt{2}}(ds - sd)s$	$-\frac{1}{\sqrt{6}}[(ds + sd)s - 2ssd]$

TABLE I: Representations of the flavor wave functions of the octet baryons.

As for  $m_\rho$ , since the value is not always provided in the lattice QCD simulations, we use the following expression based on the lattice studies made in Ref. [122],

$$m_\rho = a_0 + a_2 m_\pi^2, \quad (4.30)$$

where  $m_\pi$  is the value of the pion mass used in the lattice QCD simulation,  $a_0 = 0.766$  GeV and  $a_2 = 0.427$  GeV $^{-1}$ .

With the procedure explained above, we can associate our model with a lattice QCD simulation with the same  $m_\pi$  (lattice QCD regime).

## V. VALENCE QUARK CONTRIBUTIONS FOR THE NUCLEON

We present in this section the expressions for the nucleon axial-vector and induced pseudoscalar form factors associated with the different valence quark contributions of the nucleon wave function. Since the nucleon wave function (4.9) is a combination of the  $S$ - and  $P$ -states, the contributions for the axial current (4.5) can be decomposed into an  $S$ -state term ( $\propto n_S^2$ ), an  $S \rightarrow P$  term ( $\propto n_S n_P$ ) and a  $P$ -state term ( $\propto n_P^2$ ), as presented in the next sections. The individual contributions for the form factors associated with the transitions between the  $S$ - and  $P$ -states,  $S \rightarrow S$ ,  $S \leftrightarrow P$  and  $P \rightarrow P$ , will be represented by the upper indices  $SS$ ,  $SP$  and  $PP$ , respectively. Note that, the transition between the  $S$ - and  $P$ -states is possible due to the structure of the axial current,  $\gamma^\mu \gamma_5$ . However, in the limit  $Q^2 = 0$  the  $SP$  contribution vanishes (the same happens for the current given by a Dirac term  $\gamma^\mu$ ).

In order to present the results in a covariant form, we introduce some useful notation below. For the average momentum between the initial and final momenta we use

$$P' = \frac{1}{2}(P_+ + P_-). \quad (5.1)$$

Then  $(P')^2$  can be written as  $(P')^2 = M^2(1 + \tau)$ , with  $\tau = \frac{Q^2}{4M^2}$ . It is also convenient to define

$$\tilde{k}' = k - \frac{P' \cdot k}{(P')^2} P'. \quad (5.2)$$

In the Breit frame  $\tilde{k}'$  is reduced to the spacial component,  $\tilde{k}' = (0, \mathbf{k})$ , and  $(\tilde{k}')^2 = -\mathbf{k}^2$ .

The analytic expressions for the transition form factors, to be given next, can be expressed in terms of a few invariant integrals defined by the factors:

$$a = \frac{P' \cdot k}{M}, \quad (5.3)$$

$$c_0 = \frac{(P' \cdot k)^2}{(P')^2}, \quad (5.4)$$

$$c_1 = -(\tilde{k}')^2, \quad (5.5)$$

$$c_2 = -\frac{(q \cdot k)^2}{q^2}. \quad (5.6)$$

In the Breit frame one has  $a = \sqrt{1 + \tau} E_D$ ,  $c_0 = E_D^2$ ,  $c_1 = \mathbf{k}^2$  and  $c_2 = k_z^2$ , where  $E_D = \sqrt{m_D^2 + \mathbf{k}^2}$  and  $k_z$  is the  $z$ -component of the three-momentum  $\mathbf{k}$ .

### A. $S$ -state

The  $S$ -state contribution for the form factors can be expressed as

$$G_A^{SS}(Q^2) = \frac{5}{3} n_S^2 g_A^q(Q^2) B_0(Q^2), \quad (5.7)$$

$$G_P^{SS}(Q^2) = \frac{5}{3} n_S^2 g_P^q(Q^2) B_0(Q^2), \quad (5.8)$$

where  $n_S^2 = 1 - n_P^2$ , and

$$B_0(Q^2) = \int_k \psi_S(P_+, k) \psi_S(P_-, k), \quad (5.9)$$

is the nucleon *Body form factor*. This calculation can be done using the  $S$ -state model from Ref. [98].

In the limit  $n_S^2 = 1$  and  $g_A^q(0) = 1$  we obtain the result of the static quark model (or naive quark model)  $G_A(0) = \frac{5}{3}$  [12, 13, 27, 39, 42, 50, 57, 123]. The inclusion of relativistic corrections on nonrelativistic models reduces the value of  $G_A(0) = \frac{5}{3}$ , to a value closer to the experimental value  $G_A(0) \simeq 1.27$  [12, 31, 39, 123].

The result  $G_A(0) = \frac{5}{3}g_A^q(0)$ , implies that if we want to explain the experimental value within a simplified model, we need to admit that the axial charge of the quark is smaller than the unit,  $g_A^q(0) < 1$ , breaking the connection with the electromagnetic isovector current [ $g_A^q(0) \neq f_{1-}(0)$ ]. Similar effects were already observed in other frameworks [13, 35, 38, 39, 41, 52, 123]. Calculations based on the Dyson-Schwinger formalism suggests that the quark axial-vector coupling  $g_A^q(0)$  is reduced relatively to  $g_A^q(0) = 1$ , due to the gluon dressing of the quarks [38, 39, 41].

### B. Transition between $S$ - and $P$ -states

For the  $S$ - to  $P$ -state and the  $P$ - to  $S$ -state transitions we obtain, using  $n_{SP} = n_S n_P$ ,

$$G_A^{SP}(Q^2) = -\frac{10}{3}n_{SP}\frac{\tau}{1+\tau}g_A^q(Q^2)B_1(Q^2), \quad (5.10)$$

$$G_P^{SP}(Q^2) = -\frac{10}{3}n_{SP}\left[\frac{1}{1+\tau}g_A^q(Q^2) + g_P(Q^2)\right]B_1(Q^2), \quad (5.11)$$

where

$$B_1(Q^2) = \int_k \frac{P' \cdot k}{M} \psi_P(P_+, k) \psi_S(P_-, k). \quad (5.12)$$

Note that in the Breit frame  $\frac{P' \cdot k}{M} = E_D \frac{E_N}{M}$ , with  $E_N = M\sqrt{1+\tau}$  being the nucleon energy (initial or final state).

### C. $P$ -state

The results for the  $P$ - to  $P$ -state transition is given by

$$G_A^{PP}(Q^2) = \frac{4}{3}n_P^2 g_A^q(Q^2) \times [\tau B_2(Q^2) - (1+\tau)B_4(Q^2)], \quad (5.13)$$

$$G_P^{PP}(Q^2) = \frac{5}{3}n_P^2 g_A^q(Q^2) \times \left[ \frac{B_5(Q^2)}{\tau} + 2B_2(Q^2) - 2B_4(Q^2) \right] + \frac{5}{3}n_P^2 g_P(Q^2) \times [\tau B_2(Q^2) + B_3(Q^2) - (2+\tau)B_4(Q^2)], \quad (5.14)$$

where

$$B_2(Q^2) = \int_k \frac{(P' \cdot k)^2}{(P')^2} \psi_P(P_+, k) \psi_P(P_-, k), \quad (5.15)$$

$$B_3(Q^2) = \int_k (-\tilde{k}'^2) \psi_P(P_+, k) \psi_P(P_-, k), \quad (5.16)$$

$$B_4(Q^2) = \int_k \frac{(q \cdot k)^2}{Q^2} \psi_P(P_+, k) \psi_P(P_-, k), \quad (5.17)$$

$$B_5(Q^2) = \int_k (2S_3) \psi_P(P_+, k) \psi_P(P_-, k). \quad (5.18)$$

In the last equation,  $2S_3 = \frac{q^2 \tilde{k}'^2 - 3(q \cdot k)^2}{q^2}$ . Note that the integrals (5.15)-(5.18) can be reduced to simpler forms in the Breit frame, according to Eqs. (5.3)-(5.6).

The function  $B_5$  can also be represented as  $B_5 = B_3 - 3B_4$ . However, it is convenient to define  $B_5$  as an independent function, since  $B_5 \propto \tau$  for small  $\tau$ , which implies that  $\frac{B_5}{\tau} \rightarrow \text{constant}$  when  $Q^2 \rightarrow 0$ . This property is the consequence of the result,  $S_3 = |\mathbf{k}| \sqrt{\frac{16\pi}{5}} Y_{20}(\hat{k})$  when  $Q^2 \rightarrow 0$ . Note that the factor  $Y_{20}(\hat{k})$  is associated with  $L = 2$  transitions between the two  $P$ -state components in the nucleon wave function.

### D. Summary of the valence quark contributions

We discuss now the total contribution from the baryon core (bare) given by the sum of the components presented below:

$$G_A^B(Q^2) = G_A^{SS}(Q^2) + G_A^{SP}(Q^2) + G_A^{PP}(Q^2), \quad (5.19)$$

$$G_P^B(Q^2) = G_P^{SS}(Q^2) + G_P^{SP}(Q^2) + G_P^{PP}(Q^2). \quad (5.20)$$

Using the result for  $G_A^B$ , we can estimate the amount of  $P$ -state mixture  $n_P$  in terms of the value of  $G_A^B(0)$ , in the case where there are no meson cloud contributions. From the normalization of the radial wave functions, we can conclude that  $B_1(0) = B_3(0) = 3B_4(0)$ . Since at  $Q^2 = 0$  the  $SP$  term vanishes, we can conclude that,

$$G_A^B(0) = \frac{15 - 19n_P^2}{9} g_A^q(0). \quad (5.21)$$

Then, if  $g_A^q(0) = 1$  as already discussed, we may estimate the  $P$ -state mixture in terms of the valence quark contribution  $G_A^B(0)$  as  $n_P = \pm \sqrt{[15 - 9G_A^B(0)]/19}$ . When  $G_A^B(0) = 1.1, \dots, 1.2$  we obtain  $n_P = \pm 0.47, \dots, \pm 0.52$ .

The improvement of the agreement with the data due to the inclusion of angular momentum components beyond the  $S$ -state approximation, was observed long time ago in the context of nonrelativistic quark models [123] and in CBM [42]. In CBM the reduction of  $G_A(0)$  from the value  $5/3$  is also a consequence of  $P$ -state, associated with the lower components of the quark Dirac spinors [42].

It is important to recall at this point that in lattice QCD simulations with large  $m_\pi$ , the contribution of the

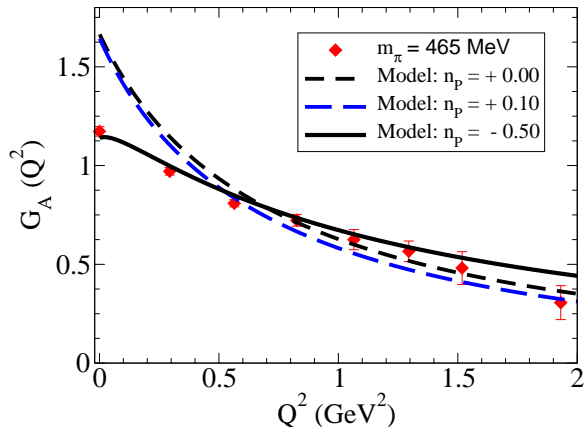


FIG. 1: Model result of  $G_A^B$  in the lattice QCD regime ( $m_\pi = 465$  MeV) for values of  $n_P = 0.0, 0.1,$  and  $-0.5$ . Lattice data are from Ref. [82].

meson cloud effects to the form factors are expected to be small, therefore  $G_A \simeq G_A^B$ . It can be then very interesting to compare the results of the extended model for the lattice QCD regime (without meson cloud) as discussed in Sec. IV E, directly with the lattice QCD data.

In Fig. 1 we compare the results of our model extended for the lattice QCD regime with the lattice QCD simulation for  $m_\pi = 465$  MeV from Ref. [82]. We can see that the pure  $S$ -state ( $n_P = 0$ ; short-dashed line), fails to describe the data for the small  $Q^2$  region, although it approaches the lattice data for large  $Q^2$ . The result for  $n_P = 0.1$  (long dash line) overestimates the data in the small  $Q^2$  region, while in the large  $Q^2$  region it underestimates. Finally, the result for  $n_P = -0.5$  (solid line) gives an excellent description of the lattice QCD data. This suggests that a mixture between the  $S$ - and  $P$ -states of about 25% with a negative coefficient ( $n_P \simeq -0.5$ ) is adequate to describe the lattice QCD data for  $G_A$  obtained with large  $m_\pi$ .

The result of the systematic study of the lattice QCD data for the range  $m_\pi = 350$ – $500$  MeV, for both form factors,  $G_A$  and  $G_P$ , will be presented in Sec. IX. In the next section we extend the formalism developed here for the nucleon to the octet baryons using the  $SU_F(3)$  flavor symmetry at the quark level.

Since in the physical regime, contrarily to the lattice QCD regime with large  $m_\pi$ , the effect of the meson cloud (in particular the pion cloud) cannot be ignored for the nucleon as well as for the other octet baryon members, in Sec. VII we discuss how the results for the physical case can be corrected by the effect of the meson cloud on the octet baryon wave functions.

## VI. VALENCE QUARK CONTRIBUTIONS FOR THE OCTET BARYONS

As in the case of the nucleon, we can calculate the axial form factors involving the other octet baryon members using the wave functions given in Sec. IV D. There are four main differences relatively to the nucleon case:

- we have now the  $u \leftrightarrow s$  transitions,
- the nucleon isospin wave function,  $\phi_I^0$  and  $\phi_I^1$ , are replaced by the anti-symmetric  $|M_A\rangle_B$  and symmetric  $|M_S\rangle_B$  flavor wave functions in  $SU(3)_F$ , as displayed in Table I,
- the radial wave functions  $\psi_S$  and  $\psi_P$  are replaced by functions with different momentum range parameters,
- there are in general a mass difference between the initial ( $M_B$ ) and the final ( $M_{B'}$ ) baryon states (for the nucleon the difference between the proton and neutron mass is negligible).

Contrarily to the nucleon case ( $n \rightarrow p$  transition) the difference in masses between the initial and final states can originate in principle additional terms to the structure of transition axial current (2.4), besides corrections dependent on the mass difference to the form factors  $G_A$  and  $G_P$ . In this work as a first approximation we consider the limit  $M_{B'} = M_B$  and replace those masses by the average  $M_{BB'}$ .

Except for the value of the mass ( $M$  or  $M_{BB'}$ ) we can calculate the results of the axial form factors for the octet, using the results for the nucleon modified by the flavor wave functions. Since the results for the nucleon can be divided into the diquark spin-0 contribution that goes with the mixed anti-symmetric flavor wave function  $|M_A\rangle_B$ , and the diquark spin-1 contribution that goes with the mixed symmetric flavor wave function  $|M_S\rangle_B$ . We define the symmetric ( $S$ ) and anti-symmetric ( $A$ ) transition coefficients,

$$f_X^A = {}_{B'}\langle M_A | X | M_A \rangle_B, \quad (6.1)$$

$$f_X^S = {}_{B'}\langle M_S | X | M_S \rangle_B, \quad (6.2)$$

where the operator  $X$  can be either  $I_0, I_\pm$  or  $V_\pm$ . The results of the octet transition coefficients are presented in Table II. The results for the neutral transitions  $B \rightarrow B$  defined by  $X = I_0 \equiv \lambda_3$  are presented in Table III for  $B = N, \Sigma,$  and  $\Xi$ . For  $\Lambda$  and  $\Sigma^0$  the coefficients are both zero, therefore  $G_A(Q^2) = 0$ . As explained in caption of Table III, the values are redefined to be independent of the charges of the baryons as in the nucleon case.

Using the new notation we can re-write the results for the nucleon in terms of the factor

$$\frac{3}{2} \left( f_X^A - \frac{1}{3} f_X^S \right) = \frac{5}{3}, \quad (6.3)$$

	$B \rightarrow B'$	$f_X^A$	$f_X^S$	$[G_A^B(0)]_{n_P=0}$	$G_A^B(Q^2)$
$\Delta I = 1$	$(I_+)$ $n \rightarrow p$	1	$-\frac{1}{3}$	$\frac{5}{3}$	$G_{A,N}^B$
	$(I_{\mp})$ $\Sigma^{\pm} \rightarrow \Lambda$	$\pm \frac{1}{\sqrt{6}}$	$\mp \frac{1}{\sqrt{6}}$	$\pm \frac{\sqrt{6}}{3}$	$\pm \frac{\sqrt{6}}{5} G_{A,N}^B$
	$(I_+)$ $\Sigma^- \rightarrow \Sigma^0$	$\frac{1}{\sqrt{2}}$	$\frac{1}{3\sqrt{2}}$	$\frac{2\sqrt{2}}{3}$	$\frac{2\sqrt{2}}{5} G_{A,N}^B$
	$(I_+)$ $\Xi^- \rightarrow \Xi^0$	0	$\frac{2}{3}$	$-\frac{1}{3}$	$-\frac{1}{5} G_{A,N}^B$
$\Delta S = 1$	$(V_+)$ $\Lambda \rightarrow p$	$-\frac{2}{\sqrt{6}}$	0	$-\sqrt{\frac{3}{2}}$	$-\frac{3\sqrt{3}}{5\sqrt{2}} G_{A,N}^B$
	$(V_+)$ $\Sigma^- \rightarrow n$	0	$-\frac{2}{3}$	$\frac{1}{3}$	$\frac{1}{5} G_{A,N}^B$
	$(V_+)$ $\Sigma^0 \rightarrow p$	0	$-\frac{\sqrt{2}}{3}$	$\frac{1}{3\sqrt{2}}$	$\frac{1}{5\sqrt{2}} G_{A,N}^B$
	$(V_+)$ $\Xi^- \rightarrow \Lambda$	$-\frac{1}{\sqrt{6}}$	$-\frac{1}{\sqrt{6}}$	$-\frac{1}{\sqrt{6}}$	$-\frac{\sqrt{3}}{5\sqrt{2}} G_{A,N}^B$
	$(V_+)$ $\Xi^- \rightarrow \Sigma^0$	$\frac{1}{\sqrt{2}}$	$-\frac{1}{3\sqrt{2}}$	$\frac{5}{3\sqrt{2}}$	$\frac{1}{\sqrt{2}} G_{A,N}^B$
	$(V_+)$ $\Xi^0 \rightarrow \Sigma^+$	1	$-\frac{1}{3}$	$\frac{5}{3}$	$G_{A,N}^B$

TABLE II: Coefficients  $f_I^{S,A}$  and  $f_V^{S,A}$  for the octet baryon transitions.

$B$	$f_X^A$	$f_X^S$	$[G_A^B(0)]_{n_P=0}$	$G_A^B(Q^2)$
$N$	1	$-\frac{1}{3}$	$\frac{5}{3}$	$G_{A,N}^B$
$\Sigma$	1	$\frac{1}{3}$	$\frac{4}{3}$	$\frac{4}{5} G_{A,N}^B$
$\Xi$	0	$\frac{2}{3}$	$-\frac{1}{3}$	$-\frac{1}{3} G_{A,N}^B$

TABLE III: Coefficients  $f_{I_0}^{S,A}$  for the neutral transitions. In order to compare with the literature we correct the results for  $f_{I_0}^{S,A}$  by an isospin factor. In the case of the nucleon and  $\Xi$  the factor is the isospin projection of the baryon (+ for  $p$ ,  $\Xi^0$  and - for  $n$ ,  $\Xi^-$ ). For the  $\Sigma$  case the factor is taken as the  $\Sigma$  charge (+, 0, -).

since the nucleon case we have  $f_{I_+}^A = 1$  and  $f_{I_+}^S = -\frac{1}{3}$ . The difference in the calculation relatively to the nucleon case, apart the mass, is that the factor due to the spin structure in the nucleon case given by  $f_{I_+}^A - \frac{1}{3}f_{I_+}^S = \frac{10}{9}$ , should be replaced by the factor  $f_X^A - \frac{1}{3}f_X^S$  in the general case. Therefore, we can obtain the results of the axial form factors for the octet baryons multiplying the nucleon results by  $\frac{9}{10}(f_X^A - \frac{1}{3}f_X^S)$ .

Then, assuming that the baryon wave functions of  $B$  and  $B'$  are also defined with the mixture coefficients  $n_S$  and  $n_P$ , we can write the transition form factors with  $n_S$ ,  $n_{SP}$  and  $n_P$  in general:

$$G_A^B(Q^2) = g_A^q \mathcal{F} \left\{ \frac{3}{2} n_S^2 B_0 - 3 n_{SP} \frac{\tau}{1+\tau} B_1 + \frac{6}{5} n_P^2 [\tau B_2 - (1+\tau) B_4] \right\}, \quad (6.4)$$

$$G_P^B(Q^2) = g_A^q \mathcal{F} \left\{ -3 n_{SP} \frac{1}{1+\tau} B_1 + \frac{3}{2} n_P^2 \left[ \frac{B_5}{\tau} + 2(B_2 - B_4) \right] + \frac{M_{BB'}}{M} g_P^q \mathcal{F} \left\{ \frac{3}{2} n_S^2 B_0 - 3 n_{SP} B_1 + \frac{3}{2} n_P^2 [\tau B_2 + B_3 - (2+\tau) B_4] \right\} \right\}, \quad (6.5)$$

where one has now  $\tau = \frac{Q^2}{4M_{BB'}^2}$ , and

$$\mathcal{F} = \left( f_X^A - \frac{1}{3} f_X^S \right). \quad (6.6)$$

The effect of the mass ( $M$  or  $M_{BB'}$ ) appears in the functions  $B_i$  ( $i = 0, \dots, 5$ ).

Note in particular in Eq. (6.5) the factor  $\frac{M_{BB'}}{M}$  which corrects the quark form factor  $g_P^q$  relatively to the nucleon case. This factor is the consequence of the definition of the quark axial current given by Eq. (4.6), in terms of the nucleon mass  $M$  for *all the baryons*, in contrast to the baryonic transition currents (2.4) that depend on  $M_{BB'}$ .

For a future discussion it is important to note that the second term in the r.h.s. in Eq. (6.5) for  $G_P^B$ , the term proportional to  $g_A^q n_P^2$ , has a dependence on  $Q^2$  that is similar to the first term of the r.h.s. in Eq. (6.4) for  $G_A^B$ , for large  $Q^2$ . Both terms scale as  $1/Q^4$  for very large  $Q^2$ . This behavior is a consequence of the choice made for the radial wave functions, that enter in the definitions of the functions  $B_i(Q^2)$  ( $i = 0, \dots, 5$ ), and also from the result  $g_A^q(Q^2) \simeq \text{constant}$  in the large  $Q^2$  limit. Recall that the radial wave functions are chosen with the form of the nucleon radial wave function, and that the nucleon radial wave function is parametrized in order to describe the nucleon electromagnetic form factors for large  $Q^2$ . The consequence of this choice is that one has  $B_0(Q^2) \propto 1/Q^4$  for large  $Q^2$ , apart from some logarithmic corrections [101].



In the third columns of Tables II and III we present the result for  $G_A^B(0)$  for  $n_P = 0$ . It is interesting to look to those values, because they agree with the results of the static quark model (naive quark model), obtained also in the  $S$ -state limit. As already discussed, the covariant spectator quark model improves the result for the nucleon at  $Q^2 = 0$  when we include a  $P$ -state mixture with the value  $n_P \simeq -0.5$ .

In the last columns of Tables II and III we write the expressions obtained for the form factor  $G_A^B(Q^2)$  in terms of the result for the nucleon ( $n \rightarrow p$  transition) in the limit  $M = M_{BB'}$ , represented by the function  $G_{A,N}^B(Q^2)$ . Since the results for the octet baryons for finite  $Q^2$  are calculated under the  $SU_F(3)$  symmetry, but the symmetry is broken by the mass  $M_B$  (dependent on the isospin of the baryon), it will be interesting to see if the relations from Tables II and III expressed in terms of the result for the nucleon,  $G_{A,N}^B$ , are a good approximation for the octet baryons or not. (The parametrizations of the radial wave functions are also different for the octet baryons.) These issues will be discussed in Sec. X.

Note about the function  $G_A^B(Q^2)$  that the results are no longer related with the static quark model limit, since we now include a  $P$ -state mixture. In order to better understand the difference between the two models, the static quark model and a model with the  $P$ -state, we compare the results for the case where  $n_P \simeq -0.5$ . In the static quark model we obtain for the nucleon  $G_A^B(0) = \frac{5}{3} \simeq 1.67$ . In this case the expected result for the  $\Xi^- \rightarrow \Xi^0$  form factor is  $G_A^B(0) = -0.33$ . If we consider instead the model with the  $P$ -state discussed in Sec. V, assuming  $G_A^B(0) \simeq 1.1$  (lattice case), we obtain  $G_A^B(0) = -0.22$  for the same transition. There is therefore a significant deviation from the  $SU(6)$ .

In Sec. VIII we compare the results of our valence quark model with those of the  $SU(3)$  baryon-meson model.

## VII. MESON CLOUD EFFECTS FOR THE OCTET BARYON AXIAL FORM FACTORS

We discuss in this section how the meson cloud effects can be taken into account in the octet baryon axial form factors. We start the nucleon case. Next, we explain how the method can be extended for the other octet baryon members.

### A. Meson cloud dressing of the nucleon

Since the pion cloud is expected to be the dominant contribution in the meson cloud, we could in principle replace meson cloud by pion cloud. We will keep however the discussions general, aiming for the generalization for the octet baryons.

The meson cloud contribution can be included in the nucleon wave function using the nucleon state expanded

as

$$|N\rangle = \sqrt{Z_N} [|3q\rangle + c_N |\text{MC}\rangle], \quad (7.1)$$

where  $\sqrt{Z_N}$  is the normalization constant,  $|3q\rangle$  gives the nucleon bare (three valence quark) wave function part, and  $c_N |\text{MC}\rangle$  represents the meson cloud component associated with baryon-meson states. The coefficient  $c_N$  is determined by the normalization of the state [ $Z_N(1 + c_N^2) = 1$ , if the meson cloud component is normalized to the unit]. The component  $|3q\rangle$  has already been discussed in the previous section.

Since the nucleon wave function associated with the state (7.1) includes states beyond the valence quark core, we simply refer the state  $|N\rangle$  as the physical nucleon state [42]. Note however, that although the higher order states such as baryon-meson-meson states may also be included in the nucleon wave function by including the corresponding states in Eq. (7.1), we assume that the baryon-meson states give the more relevant corrections to the valence quark core, and ignore the higher states in this work.

We discuss now how the results obtained for the form factors due to the valence quark component are modified by the existence of the component  $|\text{MC}\rangle$ . In a framework where the baryon-meson interactions are defined by an underlying theory, we can calculate the normalization constant  $Z_N$  using the derivative of the nucleon self-energy (nucleon dressed by the meson cloud) [106, 109, 111].

Once determined  $Z_N$ , we can calculate the effective contribution of the valence quark component for a given process, including the factor  $\sqrt{Z_N}$  associated with the component  $|3q\rangle$ . Since the valence quark component itself is normalized to unity and there is a meson cloud component, we need to correct the bare contribution when we compute the effect of the valence quarks by the probability of finding a bare nucleon state (three valence quark) in the physical nucleon state  $|N\rangle$ , which will reduce the bare contribution by the factor  $(\sqrt{Z_N})^2$  due to the presence of the meson cloud.

For an easier understanding of this normalization procedure, we discuss the calculation of the proton charge  $e$ , defined by the proton Dirac form factor in the limit  $Q^2 = 0$ ,  $F_1(0)$ . Since the determination of the nucleon elastic form factors depends on the two nucleon wave functions associated with the initial and the final states, the valence quark contribution for  $F_1(0)$  which is unity, should be modified by  $Z_N = \sqrt{Z_N}\sqrt{Z_N}$  due to the normalization of the valence quark component of the wave function. Therefore only the fraction  $Z_N$  contributes to the proton charge. The remaining contribution  $(1 - Z_N)e$  is due to the meson cloud. Considering as an example the model that we will present in Sec. IX with  $Z_N = 0.73$ , we can conclude that only about 73% of the proton's charge is due to the valence quarks (27% of meson cloud).

To summarize, the contribution of the valence quarks for the axial form factor  $G_A$  can be determined from the result obtained by the bare contribution  $G_A^B$ , multiplied

by  $Z_N$ :

$$G_A^B(Q^2) \rightarrow Z_N G_A^B(Q^2). \quad (7.2)$$

See Refs [106, 109, 111] for more details.

To avoid confusion between the result for  $G_A$  obtained in the case where only the valence quarks are relevant (so far represented as  $G_A^B$ ), and the case with the meson cloud as in the physical case, we define

$$\tilde{G}_A^B(Q^2) = Z_N G_A^B(Q^2), \quad (7.3)$$

as the effective contribution of the bare core for the axial-vector form factor. Using this notation we can rewrite Eq. (3.1) as

$$G_A(Q^2) = \tilde{G}_A^B(Q^2) + G_A^{MC}(Q^2), \quad (7.4)$$

where  $G_A^{MC}$  represents, as before, the contribution of the meson cloud. Note that, as mentioned earlier, if we have a model for  $\tilde{G}_A^B$ , we can estimate  $G_A^{MC}$  phenomenologically replacing  $G_A$  by some parametrization of the experimental data.

In this work, instead of calculating  $Z_N$  from an underlying theory we chose to use the experimental data for  $G_A$  to estimate the amount of the meson cloud in the nucleon system.

Our method to estimate  $Z_N$  is the following: i) first, we calibrate our valence quark model by the lattice QCD data with large  $m_\pi$ , ii) next, we extrapolate the result for the physical limit to obtain  $G_A^B$ , iii) finally, we use Eq. (7.3) with  $\tilde{G}_B$  replaced by a phenomenological parametrization of the data for  $Q^2 > 1 \text{ GeV}^2$ , a region where the meson cloud effects are small to calculate  $Z_N$ .

Note that the estimate of the factor  $Z_N$  by the nucleon  $G_A$  form factor data, instead of just by the nucleon electromagnetic form factor data, provides in principle a more consistent estimate of the meson cloud component in the physical nucleon state  $|N\rangle$ .

## B. Meson cloud dressing of octet baryons

We assume that for the other octet baryon members we can write also an equation similar to Eq. (7.1), that includes a coefficient  $c_B$ , that is related with the normalization constant  $\sqrt{Z_B}$ . For the other octet baryon members, however, it is not possible to estimate  $Z_B$  directly from the data, since there are no data for finite  $Q^2$ . We cannot use the method based on Eq. (7.2) to estimate  $Z_B$ .

Therefore, we rely on an alternative method to estimate the normalization factor  $Z_B$  for the other octet baryon members. The method is based on the similarity between the contribution of the meson cloud for the nucleon in our model and CBM [11].

In the formalism of the covariant spectator quark model we can represent [106, 109, 111, 112]

$$Z_B = \frac{1}{1 + a_B b_1}, \quad (7.5)$$

$\sqrt{Z_N} = 0.8569$
$\sqrt{Z_\Lambda} = 0.8822$
$\sqrt{Z_\Sigma} = 0.8751$
$\sqrt{Z_\Xi} = 0.9019$

TABLE IV: Normalization factors  $\sqrt{Z_B}$  of the octet baryon wave functions as the result of the meson cloud dressing.

where  $b_1$  is a parameter that establishes the magnitude of the meson cloud in the nucleon system, and  $a_B$  is a factor dependent on the baryon flavor, constrained by  $a_N = 1$ . The coefficient  $a_B$  is defined by  $c_B^2 = a_B b_1$ , according to Eq. (7.1). Since  $a_N = 1$ , in the case of the nucleon,  $Z_N$  is determined directly by  $b_1$  and vice versa.

We compare our result for  $Z_N$  with the result of CBM [11]. Our result for  $Z_N$ , presented in Sec. IX is  $Z_N = 0.7343$ . The results from CBM is  $Z_N = 0.7114$ . We conclude therefore that the effect of the meson cloud in the nucleon wave function is very similar in both models.

Assuming that the meson cloud contribution for the octet baryon members keep the same proportion for the nucleon as in CBM, we can determine  $a_B$ , and consequently calculate  $Z_B$ . Since in the weak transitions between octet baryon members may involve different isospin multiplets in the initial and in final states, it is more convenient to present the results for  $\sqrt{Z_B}$ . The values of  $\sqrt{Z_B}$  determined by the method described above are presented in Table IV.

## VIII. $SU(3)$ BARYON-MESON MODEL

In Secs. IV, V and VI we have discussed the covariant spectator quark model which is based on the wave functions in flavor-spin space determined by the  $SU_F(3) \otimes SU_S(2)$  symmetries. In the following for simplicity we use  $SU(6)$  to represent  $SU_F(3) \otimes SU_S(2)$ .

We discuss here the results obtained by the  $SU_F(3)$  symmetry model for the hadronic weak-axial current modified by the strong interaction according to PCAC. Using the  $SU_F(3)$  symmetry we can represent the baryon-meson interactions in terms of an  $SU(3)$  chiral perturbation theory Lagrangian parametrized by three quantities, namely, the Cabibbo angle ( $\theta_C$ ), and the anti-symmetric  $F$  and the symmetric  $D$  couplings [6, 7]. Some of those models may also be referred to as the Cabibbo theory [6, 56] or the heavy baryon chiral perturbation theory [7, 57–60].

In the  $SU(3)$  baryon-meson approach, the properties of the beta decays of the octet baryons can be characterized by the couplings  $F$  and  $D$ . In particular the results for  $G_A(0)$  associated with the  $\Delta I = 1$  and  $\Delta S = 1$  octet baryon decays can be expressed in terms of  $F$  and  $D$ . The expressions for  $G_A(0)$  are presented in the column labeled as  $SU(3)$  in Table V. In Table V the signs are adjusted

according to our results for  $G_A^B(0)$  from Table II. For the discussions about the sign conventions see Refs. [4, 6, 24, 124, 125]. Also in Table V one can see, for instance, that  $G_A(0) = F + D$  for the  $n \rightarrow p$  transition and  $G_A(0) = \sqrt{2}F$  for the  $\Sigma^- \rightarrow \Sigma^0$  transition.

If we resort furthermore on the  $SU_S(2)$  symmetry we obtain the  $SU(6)$  flavor-spin symmetry. In this case:  $F = 0.4(F + D)$  and  $D = 0.6(F + D)$ . Then, all the values of  $G_A(0)$  can be determined by the value of  $F + D$  that can be fixed by the value of  $G_A(0)$  for the  $n \rightarrow p$  transition. The results for the  $SU(6)$  case are also presented in Table V [see column labeled as  $SU(6)$ ].

Note that, in the  $SU(3)$  and  $SU(6)$  approaches the dependence on the baryon masses is not reflected directly on the coupling constants  $D$  and  $F$ , which should be valid for all the weak transitions between the octet baryons ( $N, \Lambda, \Sigma, \Xi$ ). It is important to mention that although the many successful  $SU(3)$  baryon-meson models are close to the  $SU(6)$  limit of  $\alpha = F/(F + D) = 0.6$ , the two parametrizations can differ up to about 17-25%. The  $SU(3)$  baryon-meson models generally have a better agreement with the data.

It is interesting to compare the results of the  $SU(3)$  baryon-meson model in the  $SU(6)$  limit (last column in Table V) with the results of  $G_A^B$  in Table II (last column). We can conclude that the function  $G$  in Table V, and the function  $G_A^B$  in Table II, are multiplied by the same (constant) factor for a given transition. This result means that the covariant spectator quark model is equivalent to an  $SU(6)$  baryon-meson model in the limit  $Q^2 = 0$ . For the convenience of future discussions we define the relative proportion factor,  $\eta_{BB'}$ , for the axial-vector form factor for the  $B \rightarrow B'$ , relative to that of the nucleon ( $n \rightarrow p$ ).

If we estimate the contribution of the quarks  $u$  and  $d$  for the proton spin using the static quark model, we obtain  $\Delta\Sigma^u = 4/3$  and  $\Delta\Sigma^d = -1/3$ , which correspond to the total spin of the proton ( $\Delta\Sigma = 1$ ). However, the experimental value is  $\Delta\Sigma \simeq 0.33$  [8, 9], which raised the well known *proton spin crises* [8–11]. The above values of  $\Delta\Sigma^q$  correspond to  $F = \frac{2}{3}$  and  $D = 1$  [12, 13, 50, 57, 123]. In this case one has an  $SU(6)$  model ( $F = \frac{2}{3}D$ ) where  $D = 1$ . As  $F + D = \frac{5}{3}$ , we recover the results  $[G_A^B(0)]_{n_F=0}$  discussed in Sec. VI.

The  $SU(3)$  baryon-meson model gives a good description of the data when the parameters  $D$  and  $F$  are fitted to the available  $G_A(0)$  data for the octet baryons. It is important to note however that the results of the  $SU(3)$  baryon-meson model are expected to be only an approximation since the  $SU_F(3)$  symmetry is broken due to the large  $s$ -quark mass compared to the  $u$  and  $d$  quarks. The symmetry breaking due to the  $s$ -quark is indeed reflected on the variation of the octet baryon physical masses. Thus, due to the symmetry breaking, a deviation of about 20–30% from the data can be expected [6, 59, 60].

We can extend the results of the  $SU(3)$  baryon-meson model for finite  $Q^2$  replacing the constants  $F$  and  $D$  by two form factors dependent on  $Q^2$ ,  $F(Q^2)$  and  $D(Q^2)$ ,

as suggested in Ref. [6]. If we demand also  $SU(6)$  symmetry, one gets  $\alpha \equiv D(0)/(F(0) + D(0)) = 0.6$ . The results based on this, are presented in the last column of Table V in terms of  $G(Q^2) \equiv F(Q^2) + D(Q^2)$ , that is now a function of  $Q^2$ .

Note that, the difference between the calculation in Sec. VI and the  $SU(3)$  baryon-meson model extended for finite  $Q^2$ , is that the functions  $G_A^B(Q^2)$  only take into account the effect of the valence quark contributions, and the calculations of  $G(Q^2) = F(Q^2) + D(Q^2)$  are parametrized by the octet baryon beta decay data for  $Q^2 = 0$ , and the nucleon data, including finite  $Q^2$  data. Therefore the  $SU(3)$  baryon-meson model takes into account effectively all possible physical effects including the meson cloud effects.

Thus, if we consider the  $SU(3)$  baryon-meson model, with a  $Q^2$  dependence extracted from nucleon experimental data for  $G_A$ , one can estimate all the axial-vector octet baryon form factors, based on the  $SU(3)$  symmetry. However, since the baryon-meson models based on the  $SU(3)$  symmetry generally ignore the effects of the octet baryons masses in the transitions, the estimates of the  $Q^2$  dependence, except for the nucleon case, have to be taken with caution. In Sec. X we will discuss the expected falloff with  $Q^2$  according to the  $SU(6)$  baryon-meson model, and compare it with the results of the covariant spectator quark model.

Recall that, since the  $SU(3)$  and the  $SU(6)$  baryon-meson models are based on the  $SU_F(3)$  symmetry, we obtain results only in a first order (equal mass limit of the octet baryons), and a deviation from the data can be expected, even with an effective inclusion of the meson cloud effects. Corrections due to the  $SU(3)$  symmetry breaking, as the result of the large  $s$ -quark mass as well as the corrections from meson loops can be calculated using the formalism of chiral perturbation theory [57–59, 85]. It is known that meson loop corrections do not satisfy the  $SU(3)$  symmetry [57, 58]. The explicit calculation of the next leading order corrections of the  $SU(6)$  baryon-meson model are, however, beyond the scope of the present work.

Here, we emphasize that, in general, the inclusion of the meson cloud contributions breaks the  $SU(6)$  symmetry observed for the valence quark component of  $G_A$  (in the equal mass limit). However, as far as the valence quark contribution is dominant, and the coefficients  $F$  and  $D$  are fitted to the  $G_A(0)$  data, it is expected that an  $SU(3)$  or an  $SU(6)$  baryon-meson model gives a good description of the data for small  $Q^2$ . As for finite  $Q^2$ , in particular for large  $Q^2$ , it is still necessary to check if the  $SU(3)$  or  $SU(6)$  description is good, or if the effect of the octet baryon masses (symmetry breaking) is important.

For simplicity and consistency with the approximate structure of the  $SU(6)$  symmetry in the covariant spectator quark model, we will start by analyzing the meson cloud contribution with an  $SU(6)$  parametrization. This parametrization has no adjustable parameters once the contribution of the meson cloud in the nucleon axial-

	Process	$SU(3)$	$SU(6)$
$\Delta I = 1$	$n \rightarrow p$	$F + D$	$G$
	$\Sigma^\pm \rightarrow \Lambda$	$\pm\sqrt{\frac{2}{3}}D$	$\pm\frac{\sqrt{6}}{5}G$
	$\Sigma^- \rightarrow \Sigma^0$	$\sqrt{2}F$	$\frac{2\sqrt{2}}{5}G$
	$\Xi^- \rightarrow \Xi^0$	$F - D$	$-\frac{1}{5}G$
$\Delta S = 1$	$\Lambda \rightarrow p$	$-\sqrt{\frac{3}{2}}(F + \frac{1}{3}D)$	$-\frac{3\sqrt{3}}{5\sqrt{2}}G$
	$\Sigma^- \rightarrow n$	$-F + D$	$\frac{1}{5}G$
	$\Sigma^0 \rightarrow p$	$-\frac{1}{\sqrt{2}}(F - D)$	$\frac{1}{5\sqrt{2}}G$
	$\Xi^- \rightarrow \Lambda$	$-\sqrt{\frac{3}{2}}(F - \frac{1}{3}D)$	$-\frac{\sqrt{3}}{5\sqrt{2}}G$
	$\Xi^- \rightarrow \Sigma^0$	$\frac{1}{\sqrt{2}}(F + D)$	$\frac{1}{\sqrt{2}}G$
	$\Xi^0 \rightarrow \Sigma^+$	$F + D$	$G$

TABLE V: Octet baryon axial-vector form factors  $G_A(Q^2)$ , expressed in terms of  $F$  and  $D$  of  $SU(3)$  scheme, and in the case of  $SU(6)$  symmetry [6, 54].  $F$  and  $D$  here are functions depending on  $Q^2$ . In the last column  $G = F + D$  is also a function dependent on  $Q^2$ .

	$SU(3)$	$SU(6)$
$N$	$F + D$	$G$
$\Sigma$	$-\sqrt{2}F$	$-\frac{2\sqrt{2}}{5}G$
$\Xi$	$-(F - D)$	$-\frac{1}{5}G$

TABLE VI: Neutral current axial-vector form factors. As in Table V,  $G = F + D$ .

vector form factors are fixed. Later on we discuss an  $SU(3)$  parametrization where we adjust one parameter by the  $G_A(0)$  data of the octet baryons. Our results for  $G_A(Q^2)$  will be presented in Sec. X.

All the discussions in this section have been centered on the functions  $G_A$ . As for the induced pseudoscalar form factors  $G_P$ , there are no predictions from the  $SU(3)$  baryon-meson model [6, 43].

## IX. RESULTS FOR THE NUCLEON AXIAL FORM FACTORS

In this section we present our results for the nucleon axial form factors. We divide the presentation in three steps:

- Determination of the  $P$ -state mixture parameter ( $n_P$ ) in the nucleon wave function by a direct fit to the lattice QCD data for  $G_A$ .
- Determination of the quark form factor  $g_P$  by a fit to the lattice QCD data for  $G_P$ .
- Extrapolation of the model from the lattice QCD regime to the physical regime in order to obtain the valence quark contribution for the nucleon axial-

$m_\pi(\text{MeV})$	$a(\text{fm})$	$L(\text{fm})$	Ref.
373.0	0.082	2.60	[81]
377.0	0.089	2.10	[82]
403.5	0.070	2.13	[82]
431.9	0.089	2.10	[82]
465.3	0.070	2.13	[82]
467.5	0.089	2.10	[82]
469.8	0.056	2.39	[82]

TABLE VII: Parameters associated with the lattice QCD data used in the fits.  $a$  is the lattice space and  $L$  is the lattice length that defines the lattice volume  $L^3$ .

$m_\pi(\text{GeV})$	$m_N(\text{GeV})$	$m_\rho(\text{GeV})$	$\chi^2(G_A)$	$\chi^2(G_P)$
0.3730	1.2100	0.8355	1.699	2.138
0.3770	1.2225	0.8367	0.475	0.489
0.4035	1.2527	0.8456	1.038	2.164
0.4319	1.2828	0.8557	1.943	2.277
0.4653	1.3289	0.8685	1.447	0.888
0.4675	1.3343	0.8694	1.650	1.158
0.4698	1.3390	0.8703	0.402	0.318
			1.285	1.444

TABLE VIII: Masses associated with the lattice QCD data used in the fits.  $\chi^2(G_A)$  is the partial  $\chi$  squared in the fit of  $n_P$  ( $G_A$  data).  $\chi^2(G_P)$  is the partial  $\chi$  squared in the fit of  $\alpha, \beta$  to the  $G_P$  data.

vector form factor ( $G_A^B$ ). The normalization constant  $Z_N$  is determined by the fit of the  $\tilde{G}_A^B$  to the nucleon physical data  $G_A^{\text{exp}}$  according to Eq. (7.3).

In this section the masses  $m_\pi, m_\rho$  and  $m_N$  refer to the pion,  $\rho$  and nucleon masses obtained in lattice QCD simulations. In particular, for the nucleon we use  $m_N$  to avoid the confusion with the physical mass of the nucleon  $M$ .

### A. Axial-vector form factor ( $G_A$ )

The calculation of  $G_A$  is done using the expressions discussed in Sec. V, summarized in Eq. (5.19), where all the terms are function of the  $P$ -state mixing parameter  $n_P$  (since  $n_S = \sqrt{1 - n_P^2}$ ). In Sec. VD we have already shown that some lattice QCD data are well described by a  $P$ -state mixture with  $n_P \simeq -0.5$ .

Lattice QCD simulations of the axial-vector form factor of the nucleon for  $Q^2 = 0$  can be found in Refs. [69–77]. The results from Refs. [74–76] are obtained near the physical point or at the physical point. Recent calculations of  $G_A$  as a function of  $Q^2$  can be found in Refs. [78–82, 84]. Concerning the calculations of  $G_A$  for small  $Q^2$ , it is important to mention that lattice simulations per-



formed with small volumes underestimates the value of  $G_A$  [73, 78, 79]. Therefore in our study we select datasets with large volumes.

The lattice QCD data included in our fit correspond to those from Refs. [81, 82], in the pion mass range  $m_\pi = 350\text{--}500$  MeV (large  $m_\pi$ ), where only the valence quark degrees of freedom are relevant. The parameters used in the lattice simulations: the lattice space ( $a$ ) and the length  $L$  that defines the volume, are listed in Table VII. In addition to the large volumes the chosen datasets have values of  $G_A(Q^2)$  up to  $Q^2 = 2$  GeV<sup>2</sup>, which is convenient if we want to study the large  $Q^2$  region.

In Table VIII we also present the results for  $m_N$  given by the respective lattice QCD simulations, and the values of  $m_\rho$  determined by Eq. (4.30). These mass values are necessary to calculate the quark axial current (4.6) based on the VMD parametrizations discussed in Sec. IV B for the model in the lattice regime. Furthermore,  $m_N$  is also necessary to obtain the nucleon radial wave functions in the lattice regime. In the fits, to avoid the contamination of lattice QCD artifacts that may appear for large  $Q^2$ , we use only the data with  $Q^2 < 1.6$  GeV<sup>2</sup>. Above this  $Q^2$  range, the lattice QCD data are often affected by large errorbars and may show unexpected oscillations.

The results of our  $\chi^2$  per datapoint are presented in Table VIII, in the column indicated  $\chi^2(G_A)$ . By the fit we obtain the value

$$n_P = -0.5067. \quad (9.1)$$

The results of the fit are presented in Fig. 2. In the bottom panel we show the results for the heavier pion cases  $m_\pi = 465, 468, 470$  MeV, while the results for  $m_\pi = 403, 432$  MeV are in the middle panel, and the results for the lightest cases  $m_\pi = 373, 377$  MeV are in the top panel.

In Fig. 2 one can confirm that the model in the lattice QCD regime gives a very good description of the lattice data [see also the  $\chi^2(G_A)$  results in Table VIII]. In the case  $m_\pi = 432$  MeV, however, we can notice that the lattice data falloff is faster than the model (fit), and this is reflected in the large partial  $\chi^2$  value. Nevertheless, the data are still consistent with the model.

### B. Induced pseudoscalar form factor ( $G_P$ )

With the value of  $n_P$  fixed by the lattice  $G_A$  data, we can test now if the lattice  $G_P$  data can be described by a parametrization of  $g_P$  based on the VMD mechanism. We decompose  $G_P$  as  $G_P = G_A^B + G_P^{\text{pole}}$ , where the pole term is defined by Eq. (3.3), and fit the coefficients  $\alpha$  and  $\beta$  in the function  $g_P$  given by Eq. (4.8) to the lattice QCD data for  $G_P$ . The values obtained from the best fit are,  $\alpha = -3.901$  and  $\beta = 0.3297$ . The quality of the fit for each lattice dataset is presented in the column  $\chi^2(G_P)$  in Table VIII.

In Fig. 3 we show the results of the fit for three groups of pion masses discussed previously. In any case we have a

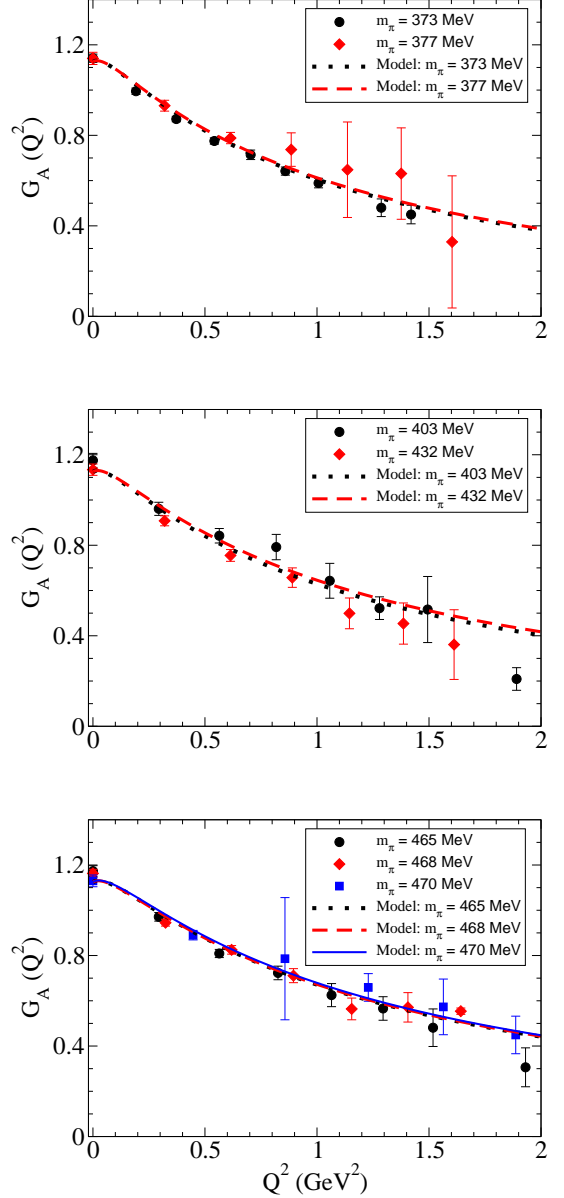


FIG. 2: Results of the fit to the lattice QCD data for  $G_A$  with  $n_P \simeq -0.5067$ .

good description of the data. (The datapoint for  $Q^2 = 0$  for  $m_\pi = 373$  MeV is the result of an extrapolation and is not included in the fit).

### C. Extrapolation to the physical regime

The experiments related with the form factor  $G_A$  show that the value for  $Q^2 = 0$  is very well determined [24]:

$$G_A^{\text{exp}}(0) = 1.2723 \pm 0.0023. \quad (9.2)$$

The  $Q^2$  dependence of  $G_A$  is well approximated by a dipole form,  $G_A(Q^2) = G_A(0)/(1 + Q^2/M_A^2)^2$ , where the

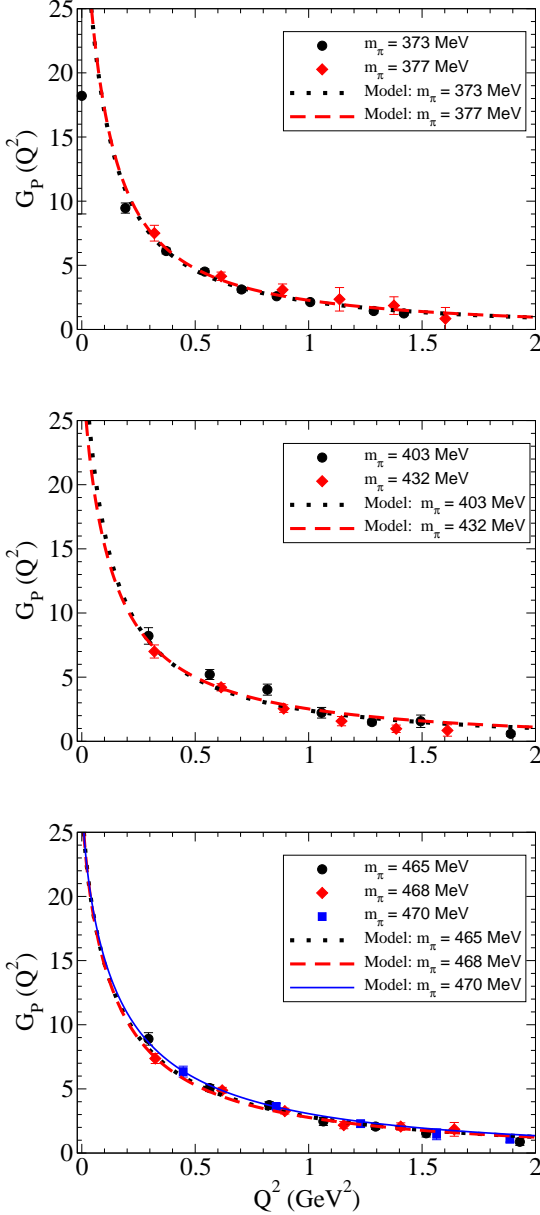


FIG. 3: Results of the fit to the lattice QCD data for  $G_P$ . The result of  $G_P(0)$  for  $m_\pi = 373$  MeV [81] is an extrapolation from the data.

values of  $M_A$  varies from  $M_A \simeq 1.03$  GeV (neutrino scattering) to  $M_A \simeq 1.07$  GeV (electroproduction) [2].

To represent the experimental data in a general form we consider the interval between the two functions,  $G_A^{\text{exp-}}$  and  $G_A^{\text{exp+}}$ , given by

$$G_A^{\text{exp}\pm}(Q^2) = \frac{G_A^0(1 \pm \delta)}{\left(1 + \frac{Q^2}{M_{A\pm}^2}\right)^2}, \quad (9.3)$$

where  $\delta$  is a parameter that expresses the precision of the data, and  $M_{A-} = 1.0$  GeV and  $M_{A+} = 1.1$  GeV are respectively the lower and upper limits for  $M_A$  extracted

experimentally. To avoid a strong impact from the result for  $Q^2 = 0$  and flexibilize the fit, we choose  $\delta \simeq 0.03$ , a typical relative error (error of about 3% and 10 times the relative error for  $Q^2 = 0$ ).

As mentioned already, the prediction of the model for the valence quark contribution is given by  $Z_N G_A^B(Q^2)$ , where  $G_A(Q^2)$  is the extrapolation for the case  $m_\pi = 138$  MeV of the model determined by the fit to the lattice QCD data (see previous section). Since the valence quark model, extrapolated to the physical regime is expected to be a good approximation to the data only for large  $Q^2$  (small meson cloud effects), we varied the value of  $Z_N$  to see if it is possible to obtain a good description of the data in the interval  $Q^2 = 1.0, \dots, 2.0$  GeV<sup>2</sup>. From the best fit to the data we obtain the value of  $Z_N = 0.7343$ . This result means that the meson cloud contribution for the proton charge is about 27%.

In Fig. 4 we present the bare contribution for the form factor  $G_A$  (dashed-line) determined by the value  $Z_N = 0.7343$ . The deviation from the empirical data  $G_A^{\text{exp}\pm}(Q^2)$ , represented by the red band, from the result  $\tilde{G}_A^B(Q^2)$ , can be interpreted as the result of the meson cloud effect. Since it is expected that the meson cloud effects are suppressed by the factor  $1/Q^4$  relative to that of the valence quark contributions for large  $Q^2$  according to perturbative QCD arguments [126], we parametrize the meson cloud contribution as

$$G_A^{MC}(Q^2) = Z_N \frac{G_A^{MC0}}{\left(1 + \frac{Q^2}{\Lambda^2}\right)^4}, \quad (9.4)$$

where  $\Lambda$  is a cutoff parameter and  $G_A^{MC0}$  is the relative magnitude of the meson cloud contribution for  $G_A(0)$ . Note that, according to the normalization of the nucleon wave function Eq. (7.1), both the valence and the meson cloud components are multiplied by the normalization factor  $Z_N$ . Therefore, for convenience the normalization factor  $Z_N$  is included in the definition of  $G_A^{MC}$ .

We have also tried some variations of the quadrupole expression (9.4), e.g., such as a product of dipoles, however, the quadrupole expression with  $\Lambda = \frac{1}{2}(M_{A+} + M_{A-}) = 1.05$  GeV, gives a description of the data with a quality equivalent to a product of dipoles with two adjustable cutoff parameters. We can interpret then Eq. (9.4) as one of the best parametrizations for the meson cloud, with the value of  $\Lambda$  fixed by the average cutoff from the global parametrizations of  $G_A$ , given in Eq. (9.3). The best fit from Eq. (9.4) for the data fixes  $G_A^{MC0} = 0.6077$ , leading to  $G_A^{MC}(0) = 0.4462$  (35% of meson cloud for  $G_A$  at  $Q^2 = 0$ ). The result of the combination for the bare and meson cloud contributions, is presented in Fig. 4 (solid-line).

To finalize the study of the nucleon axial form factors in the physical regime, we represent in Fig. 5 the results for the form factor  $G_P$  in comparison with the available data ( $Q^2 < 0.2$  GeV<sup>2</sup>). Since there are no physical data for  $Q^2 > 0.2$  GeV<sup>2</sup>, we compare the model also with the lattice QCD data with small pion masses

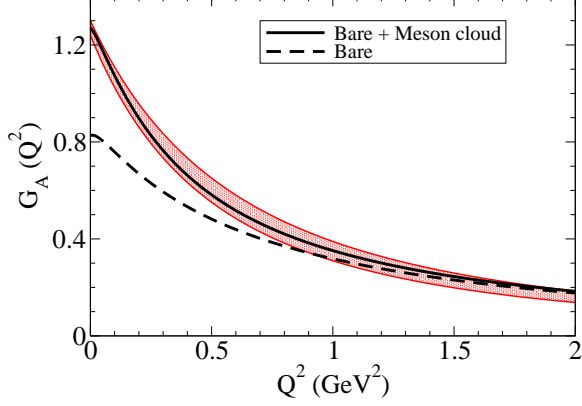


FIG. 4: Result for  $G_A(Q^2)$  in the physical limit. The dashed-line (Bare) is the result from the extrapolation of the lattice data for the physical regime with  $Z_N = 0.7434$ . The solid-line (Bare + Meson cloud) is the sum of the bare contribution with  $G_A^{MC}(Q^2)$  given by Eq. (9.4), with  $\Lambda = 1.05$  GeV. The bands are a representation of the experimental data.

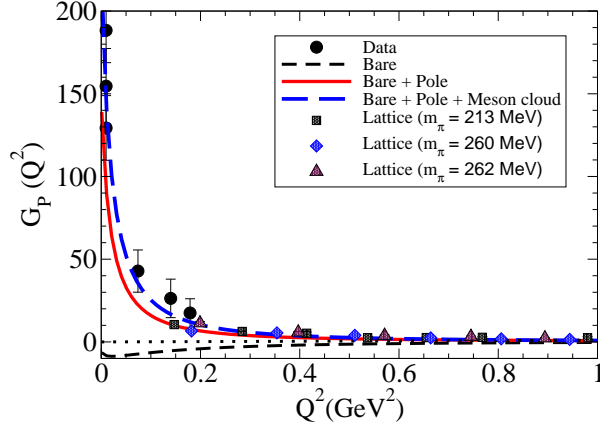


FIG. 5: Physical result for  $G_P(Q^2)$ . The data are from Refs. [2, 22]. Lattice QCD data are from Ref. [81].

$m_\pi = 213, 260, 262$  MeV. Lattice QCD data for  $G_P$  can also be found in Refs. [76, 78, 80, 84].

For the following discussion we recall that  $G_P$  can be decomposed in the physical regime into

$$G_P(Q^2) = G_P^{\text{pole}}(Q^2) + \tilde{G}_P^B(Q^2) + G_P^{MC}(Q^2), \quad (9.5)$$

where  $G_P^{\text{pole}}$  is the contribution from the pion pole defined by Eq. (3.3) in terms of bare axial-vector form factor,  $\tilde{G}_A^B$ , in the physical limit, and  $G_P^{MC}$  is a possible contribution from the meson cloud. For convenience we redefine the bare contribution  $G_P^B$  as  $\tilde{G}_P^B = Z_N G_P^B$  in the physical limit.

In Fig. 5 we represent the bare contribution by the short-dashed line. The magnitude is small and negative. The sum of the pion pole term and the bare contribution is indicated by the solid line. We can see in Fig. 5 that the line “bare + pole” (solid line) is very close

	Model	Ref. [85]	Ref.[86]
$N$	1.125	1.210(05)	1.314(24)
$\Sigma$	0.900	0.900(30)	0.970(21)
$\Xi$	-0.225	-0.270(10)	-0.300(10)

TABLE IX: Comparison of the results for the neutral current  $G_A^B(0)$  in the covariant spectator quark model and the lattice QCD results with  $m_\pi \approx 500$  MeV from Refs. [85, 86].

	Model	Ref.[86]
$n \rightarrow p$	1.125	1.314(24)
$\Sigma^+ \rightarrow \Lambda$	0.551	0.655(14)
$\Sigma^- \rightarrow \Sigma^0$	0.636	0.686(15)
$\Xi^- \rightarrow \Xi^0$	-0.225	-0.300(10)
$\Lambda \rightarrow p$	-0.827	-0.632(14)
$\Sigma^- \rightarrow n$	0.225	0.339(12)
$\Xi^- \rightarrow \Lambda$	-0.276	-0.274(08)
$\Xi^- \rightarrow \Sigma^0$	0.795	0.908(19)
$\Xi^0 \rightarrow \Sigma^+$	1.125	1.284(28)

TABLE X: Comparison of the results for  $G_A^B(0)$  in the covariant spectator quark model and the lattice QCD results with  $m_\pi \approx 500$  MeV from Ref. [86].

to physical data. In addition we show the full result, labeled as “bare + pole + meson cloud” (long-dashed line), where we define the meson cloud contribution as  $G_P^{MC} = \frac{4M^2}{m_\pi^2 + Q^2} G_A^{MC}$ . This procedure is equivalent to redefine the contribution from the pole contribution by the replacement  $\tilde{G}_A^B \rightarrow G_A$ , when no  $G_P^{MC}$  term contribution is included. In the figure we can also see that the sum of all terms “bare + pole + meson cloud” has a better agreement with the data than “bare + pole”. Note also that final result (sum of all terms) agrees with both the physical data ( $Q^2 < 0.2$  GeV<sup>2</sup>) and the lattice QCD data for larger  $Q^2$ .

Overall, we conclude that the covariant spectator quark model, once fitted to the lattice QCD data and the experimental nucleon data for  $G_A$ , gives a consistent description of the lattice and physical data for the nucleon. The fit for the  $G_A(Q^2)$  data fixes the amount of the meson cloud contribution for the physical nucleon state as 27% ( $Z_N = 0.7324$ ), resulting the meson cloud contribution for the axial-vector form factor at  $Q^2 = 0$  as 0.4462 (35% of the total), and the falloff of the meson cloud component as a quadrupole with a cutoff  $\Lambda = 1.05$  GeV.

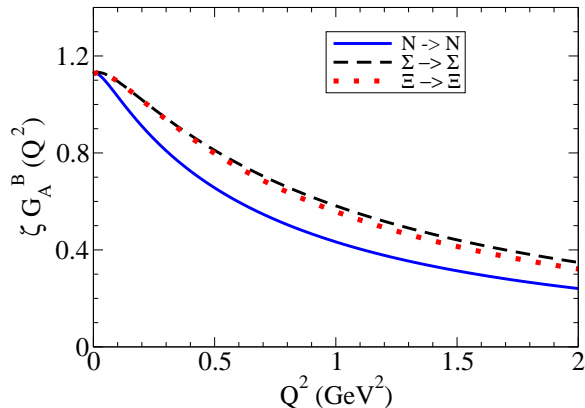


FIG. 6: Result for  $G_A^B(Q^2)$  for the octet baryon neutral current transitions normalized to the result of the nucleon at  $Q^2 = 0$ . The factor  $\zeta$  is defined as  $\zeta = G_{A,N}^B(0)/G_A^B(0)$ . Then, one has  $\zeta = 5/4$  for  $\Sigma$  and  $\zeta = -5$  for  $\Xi$ .

## X. RESULTS FOR THE OCTET BARYON AXIAL FORM FACTORS

We present now the results for the octet baryon axial form factors. First, we discuss the results for the valence quark contributions, and compare the results with those of the lattice QCD. Next, we combine the valence quark contributions with the meson cloud contribution estimated based on an  $SU(6)$  baryon-meson model, and an  $SU(3)$  baryon-meson model defined by a fit to the data. Combining the two contributions we obtain our final predictions for the octet baryon axial-vector form factors. We finish with our predictions for the octet baryon  $G_P$  form factors, based on these two models.

A note of caution is in order concerning the following results. Since the predictions of the model for the octet baryon axial form factors  $G_A$  and  $G_P$  are based on the calibration of the radial wave functions developed in Ref. [109], for the study of the octet electromagnetic form factors, the quality of the results is also limited by the numerical results in that study. Therefore, we expect the results for the reactions with the nucleon,  $\Lambda$  and  $\Sigma$  to be more reliable than that with  $\Xi$ .

### A. Contribution of valence quarks for $G_A$

We start the presentation of our results for the octet baryons discussing the effect of the valence quark contributions for the form factor  $G_A$ . Since we have not included the meson cloud contribution, it can be interesting to compare the results with the lattice QCD simulations first.

The comparison of our results with the lattice QCD simulations [85, 86] for the neutral current transitions ( $N$ ,  $\Sigma$ ,  $\Xi$ ) are presented in Table IX. The results for the  $\Delta I = 1$  and  $\Delta S = 1$  transitions compared with Ref. [86]

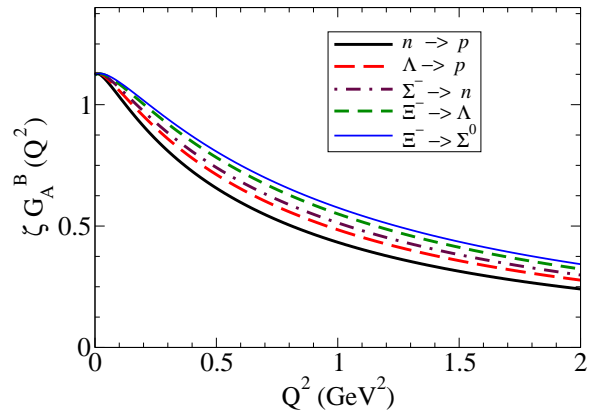


FIG. 7: Results for  $G_A^B(Q^2)$  for the octet baryon transitions with  $\Delta S = 1$  normalized to the result for the nucleon at  $Q^2 = 0$ .

are presented in Table X. To avoid any contamination from meson cloud effects, we use lattice QCD simulations with  $m_\pi \approx 500$  MeV from Refs. [85, 86] for the comparison. From Tables IX and X, one can see that the results of our model are close to the estimates of the lattice QCD.

The results of our model presented in Tables IX and X are not calculated in the lattice QCD regime, as in the case of the nucleon [see Secs. IX A and IX B]. However, this is not an approximation, since, due to the constraints of the model, the transition form factors  $G_A$  are independent of the masses for  $Q^2 = 0$  (but for  $G_P$  we have a correction). This interesting propriety is a consequence of the definition of the quark current at  $Q^2 = 0$ , independent of the hadron masses ( $m_\rho$  and  $m_N$ ), and also a consequence of the fact that the normalization of the radial wave functions is independent of the masses of the baryons (normalization defined by the wave functions at the rest frame).

We can consider a more sophisticated model where  $g_A^q(0)$  and  $g_P^q(0)$  depend on the constituent quark mass as in Ref. [102] at the expenses of an extra parameter. In that case we expect however only a small correction, as in the case of the electromagnetic transitions [102]. For the purpose of the present study, the approximation that  $g_A^q(0)$  and  $g_P^q(0)$  are independent of the constituent quark mass is sufficient.

In the calculation we use the octet baryon physical masses,  $M_N = 0.939$  GeV,  $M_\Lambda = 1.116$  GeV,  $M_\Sigma = 1.192$  GeV and  $M_\Xi = 1.318$  GeV. The values of  $M_{BB'}$  are determined using these values.

Back to the discussion of the results in Table X, our calculations are compatible with the lattice results within a  $\pm 20\%$  deviation, with two main exceptions: the  $\Sigma^- \rightarrow n$  and  $\Xi^- \rightarrow \Xi^0$  transitions. In the  $\Sigma^- \rightarrow n$  transition, the lattice value deviates also from the estimate of  $SU(3)$  baryon-meson model for the other transitions. In the case of the  $\Xi^- \rightarrow \Xi^0$  transition, the model and the lattice QCD result are both small in comparison with the other



transitions. Since we compare the core effects with lattice simulations with  $m_\pi \approx 500$  MeV, one can regard the agreement as reasonable. Looking in more detail for the result of the nucleon, we note that the model underestimates the lattice result. However, the lattice results from Ref. [86] are larger compared with similar lattice QCD simulations, like for instance, the results of Ref. [85] presented in Table IX. When the pion mass decreases, the value of  $G_A(0)$  becomes almost constant and close to the physical value, as far as the lattice volume is not too small [73, 79]. If the lattice volume becomes smaller, the lattice result for  $G_A(0)$  starts to deviate from the continuous limit, and strongly underestimates the physical result [73].

The results for the neutral transitions and  $\Delta S = 1$  transitions are presented respectively in Figs. 6 and 7. The results are normalized by the value of  $G_A^B(0)$  for the nucleon in order to better observe the differences of falloffs. The factor  $\zeta$  that multiplied to  $G_A^B(Q^2)$ , is defined by  $\zeta = G_{A,N}^B(0)/G_A^B(0)$ . We do not present a figure for the  $\Delta I = 1$  transitions, since those, with the exception of the  $\Sigma^\pm \rightarrow \Lambda$  case, are proportional to the results for the neutral transitions (see Tables IX and X). The result for  $\Sigma^+ \rightarrow \Lambda$  is very close to the  $\Xi \rightarrow \Xi$  and  $\Sigma \rightarrow \Sigma$ . The result for  $\Sigma^- \rightarrow \Lambda$  has the opposite sign to that of  $\Sigma^+ \rightarrow \Lambda$ .

In Fig. 6 one can see that the results for  $\Sigma$  and  $\Xi$  are very similar. In Fig. 7 for simplicity we do not include the line associated with  $\Sigma^0 \rightarrow p$ , because it is almost on the top of the line for  $\Lambda \rightarrow p$ , since the mass difference between  $\Sigma$  and  $\Lambda$  is small (about 80 MeV).

It is clear from Figs. 6 and 7 that the reactions with heavier baryons have slower falloffs with increasing  $Q^2$ , compared to the nucleon case. That is a consequence of using the physical masses of the baryons in the calculation instead of using the one common value of the octet baryon mass suggested by the exact  $SU(3)$  symmetry, as well as a consequence of the difference in parametrizations of the radial wave functions [see Sec. VI].

It is also interesting to note that the form factors associated with heavy baryons (excluding the nucleon) have very similar falloffs for large  $Q^2$ , although differ in the behavior in the range  $Q^2 = 0, \dots, 0.5$  GeV<sup>2</sup>

## B. Results for the axial-vector form factor ( $G_A$ )

We present now our predictions for the octet baryon  $G_A$  form factors as functions of  $Q^2$  based on the model calibrated in the previous sections by the nucleon data.

For the later discussions, it is important to mention that the results obtained up to now within the covariant spectator quark model (valence quark contribution) for  $G_A^B(0)$  correspond to an  $SU(6)$  model with parameters  $F = 0.675$  and  $D = 0.450$ . The model fails to describe the data because  $F + D$  is too small, and also because the model breaks the  $SU(6)$  symmetry for finite  $Q^2$ , as already discussed.

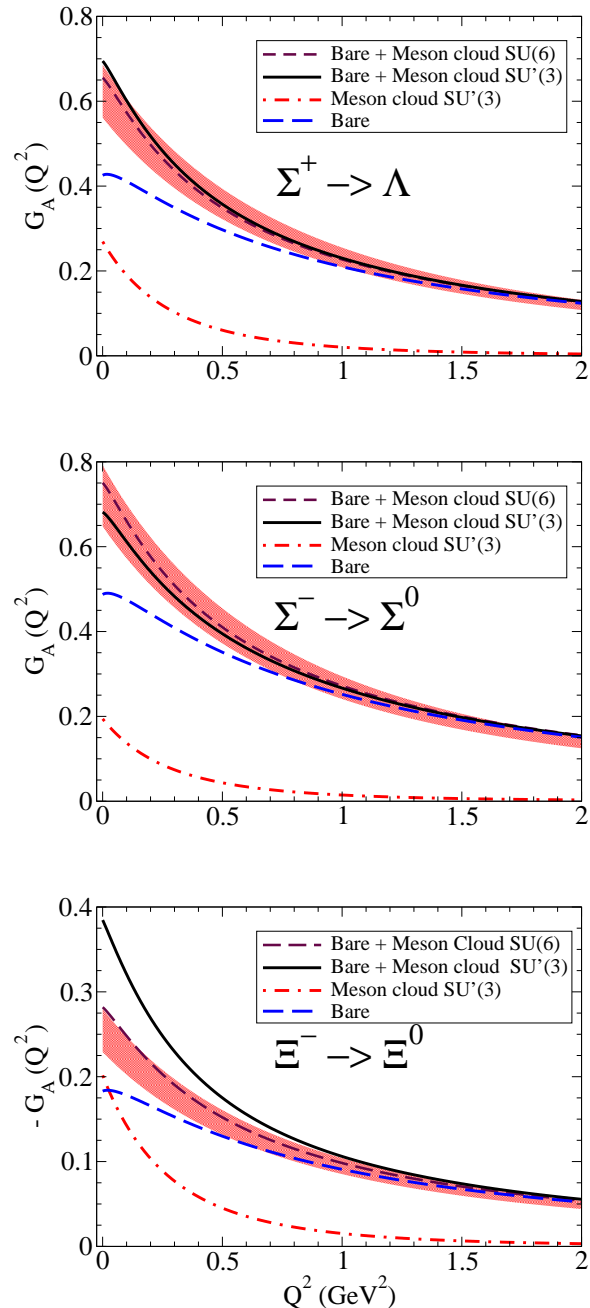


FIG. 8: Result of  $G_A(Q^2)$  for the octet baryons with  $\Delta I = 1$ . For convenience we changed the sign of the function  $G_A$  for  $\Xi^- \rightarrow \Xi^0$ .

As in the case of the nucleon, one has to correct the result from the valence quark contribution by the normalization factor due to the meson cloud. We use then

$$\tilde{G}_A^B(Q^2) = \sqrt{Z_{B'}} \sqrt{Z_B} G_A^B(Q^2), \quad (10.1)$$

where  $Z_{B'}$ ,  $Z_B$  are the normalization factors associated with the initial and final baryons.

As for the meson cloud contribution, we consider two possible parametrizations that we label as  $SU(6)$  and  $SU'(3)$  hereafter.

We first explain the  $SU(6)$  model for the meson cloud. In the  $SU(6)$  model we assume that  $SU(6)$  symmetry holds for the valence quark component of the form factors as well as the meson cloud contribution. In this case we can write the meson cloud contribution in the form

$$G_A^{MC}(Q^2) = \eta_{BB'} \frac{\sqrt{Z_{B'} Z_B}}{Z_N} G_{A,N}^{MC}(Q^2), \quad (10.2)$$

where  $G_{A,N}^{MC}$  represents the parametrization of the nucleon meson cloud contribution given by Eq. (9.4) with  $\Lambda = 1.05$  GeV. The coefficient  $\eta_{BB'}$  is the factor associated with the  $SU(6)$  symmetry, the coefficient that multiplied to  $G$  in the last column of Table V. Note that as for the nucleon, we include the normalization factors associated with the octet baryon wave functions. The factor  $1/Z_N$  is introduced to remove the dependence on the nucleon's normalization in the definition of  $G_{A,N}^{MC}$ .

Contrarily to the contribution from the valence quarks (10.1), the meson cloud contribution is independent of the baryons masses in the  $SU(6)$  model. We ignore here minor differences due to the normalization constants  $Z_B$  and  $Z_{B'}$ , since the corrections are of about 2–10%. This is a consequence of the  $SU(6)$  assumption, that the octet baryons have all the same mass.

Since  $SU(6)$  symmetry is not expected to work well in general for the meson cloud component of the form factors as discussed in Sec. VIII, we consider the possibility of improving the meson cloud model given by Eq. (10.2) by a direct fit to the data at  $Q^2 = 0$ . To achieve this goal, we use an alternative parametrization for the meson cloud, where the octet baryon data for  $G_A(0)$  are fitted by an  $SU(3)$  model for the meson cloud component. In this model the  $SU(6)$  structure for the quark model is preserved, but the meson cloud contribution is determined by an  $SU(3)$  parametrization in terms of the two coefficients denoted by  $F'$  and  $D'$ , that replace the coefficients  $F$  and  $D$  in the  $SU(3)$  baryon-meson model discussed in Sec. VIII. We break then the  $SU(6)$  symmetry in the meson cloud component. To avoid misinterpretations, we label this model as the  $SU'(3)$  model for the meson cloud.

In the  $SU'(3)$  model we write the meson cloud contribution as

$$G_A^{MC}(Q^2) = \eta'_{BB'} \frac{\sqrt{Z_{B'} Z_B}}{Z_N} G_{A,N}^{MC}(Q^2), \quad (10.3)$$

where  $\eta'_{BB'}$  represents the expressions in the column labeled as  $SU(3)$  in Table V, with the replacements  $F \rightarrow F'$ ,  $D \rightarrow D'$ , normalized by  $F' + D'$ . From the fit to the data we obtain  $F' = 0.1784$  and  $D' = 0.4273$ . The results obtained for the  $n \rightarrow p$ ,  $\Xi^- \rightarrow \Sigma^0$  and  $\Xi^- \rightarrow \Sigma^0$  transitions, where the meson cloud contributions is proportional to  $F' + D'$ , are indistinguishable from the  $SU(6)$  model. This happens because the fit is strongly constrained by the result of  $G_A(0)$  for the  $n \rightarrow p$  transition due to the high accuracy of the datapoint. Since in practice  $F' + D'$  is fixed, we fit only the relative size of the

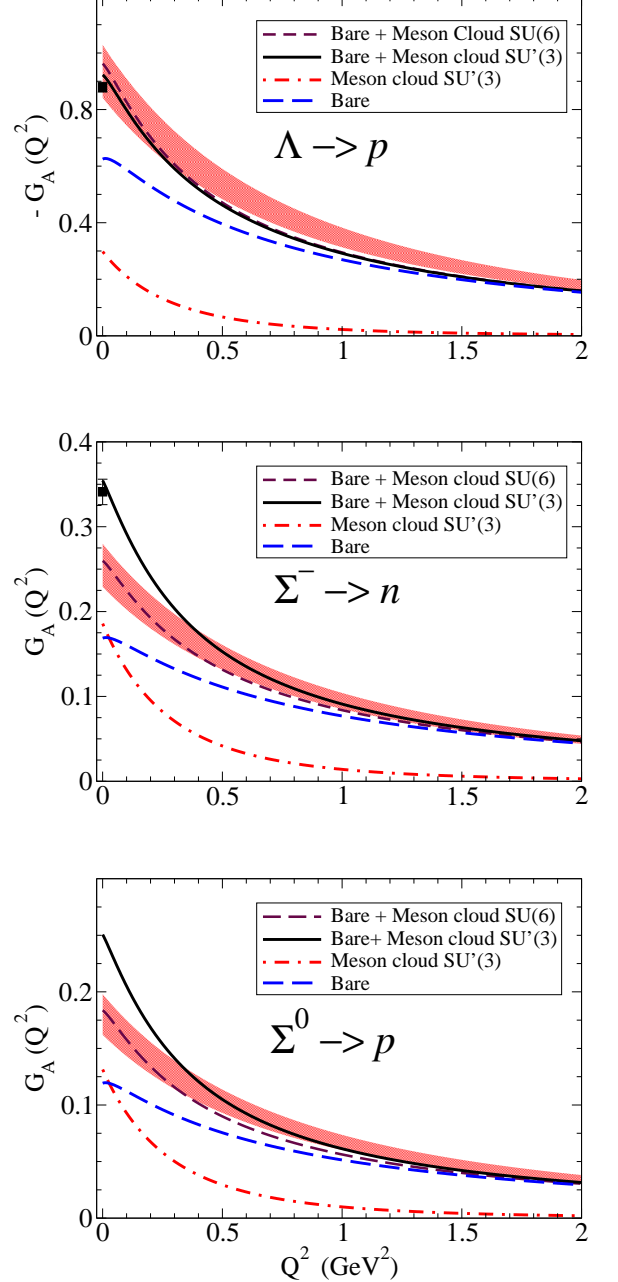


FIG. 9: Result of  $G_A(Q^2)$  for the octet baryons with  $\Delta S = 1$  (part 1). For convenience we changed the sign of the function  $G_A$  for  $\Lambda \rightarrow p$ .

coefficients  $F'$  and  $D'$ . Therefore the  $SU'(3)$  model is the result of a fit with one parameter only.

It is worth to mention that models based on the  $SU(3)$  symmetry fits to subsets of the data were used already in the past in attempts to interpret the impact of the  $SU(3)$  symmetry breaking effect [6, 43, 63].

The results for the octet baryon axial-vector form factors for  $\Delta I = 1$ , with the exception of the nucleon discussed earlier, are presented in Fig. 8. The results for

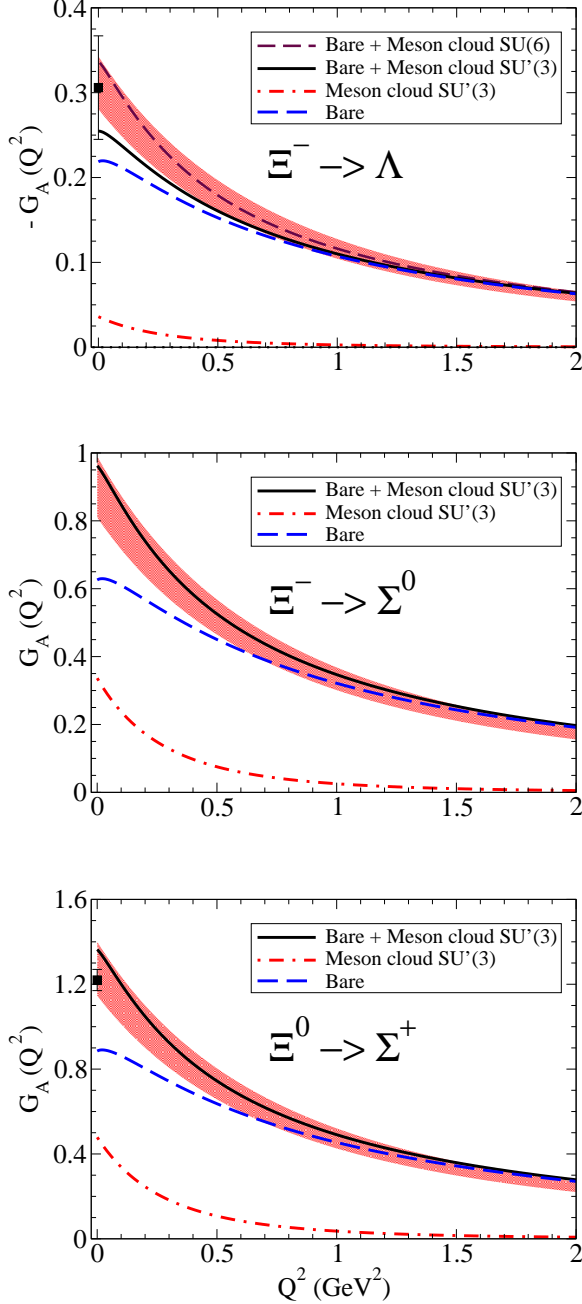


FIG. 10: Result of  $G_A(Q^2)$  for the octet baryons with  $\Delta S = 1$  (part 2). For convenience we changed the sign of the function  $G_A$  for  $\Xi^- \rightarrow \Lambda$ .

$\Delta S = 1$  are presented in Figs. 9 and 10.

In Figs. 8, 9 and 10 we include the contribution from the valence quark component (long-dashed line), the contribution from the  $SU'(3)$  model for the meson cloud (dotted-dashed line), and the final result for the model with the  $SU'(3)$  meson cloud (solid line). In addition, we present the final result (bare + meson cloud) for the  $SU(6)$  meson cloud model (short-dashed line). The meson cloud contribution of the  $SU(6)$  meson cloud model

is not presented to avoid the superposition of lines. The difference between the meson cloud components between the  $SU'(3)$  and the  $SU(6)$  models can however be estimated by the difference between the result “bare + meson cloud” in the two models. For the transitions  $\Xi^- \rightarrow \Sigma^0$  and  $\Xi^0 \rightarrow \Sigma^+$ , we omit the indication of the  $SU(6)$  model since it is equivalent to the  $SU'(3)$  model, as discussed already.

In order to compare our results with the estimates of the  $SU(6)$  baryon-meson model discussed in Sec. VIII, which are independent of the baryon masses, we present a band (at red) given by the parametrization inspired by the fit to the nucleon data,

$$G_A^{SU(6)}(Q^2) = \eta_{BB'} \frac{G_A^0}{\left(1 + \frac{Q^2}{M_A^2}\right)^2}, \quad (10.4)$$

where  $M_A$  is cutoff parameter. The band indicates a  $\pm 10\%$  variation from Eq. (10.4).

It was suggested by Gaillard and Sauvage [6] that  $M_A = 1.05$  GeV for  $\Delta I = 1$  and  $M_A = 1.25$  GeV for  $\Delta S = 1$ . Using the two different parametrizations for  $\Delta I = 1$  and  $\Delta S = 1$  we take into account in an effective way the modification due to the octet baryon mass difference in the  $SU(6)$  baryon-meson model. We realize however, that our model cannot be compared with the results of  $M_A = 1.05$  GeV for both cases,  $\Delta S = 1$  and  $\Delta I = 1$ , except for the case of the nucleon, discussed in Sec. IX A. Therefore, we compare all our estimates with  $M_A = 1.25$  GeV. At  $Q^2 = 0$ , we compare also the results with the data from Particle Data Group (PDG) [24].

We recall that, although we present different parametrizations for the meson cloud that differ at low  $Q^2$ , our results may be considered true predictions in the high  $Q^2$  region, since the result is extrapolated from the model calibrated by the lattice QCD data as well as the high  $Q^2$  data for the nucleon. In the large  $Q^2$  region the meson cloud contributions are very small and the valence quark effects dominate.

The results of both models are close to the data, but the model  $SU'(3)$  gives a better description of the  $\Sigma^- \rightarrow n$  data. Larger difference between the  $SU(6)$  and the  $SU'(3)$  parametrizations is also observed for the reactions with small magnitude for  $G_A(0)$  ( $\Xi^- \rightarrow \Xi^0$ ,  $\Sigma^- \rightarrow n$  and  $\Sigma^0 \rightarrow p$ ). This is a consequence of the large meson cloud contributions compared to those of the valence quarks. In any case, we should not expect an excellent agreement with the  $G_A(0)$  data, since the  $SU(3)$  symmetry at the quark level is already broken (based on the octet baryon masses the violation is about 20%).

In the comparison with the data at  $Q^2 = 0$  the deviation is less than five standard deviations, and better than 24% for the model  $SU(6)$ . As for the model  $SU'(3)$  the deviations is less than three standard deviations and better than 17%.

It is also interesting to note that the estimate of the meson cloud effects based on the  $SU(6)$  parametrization is in general larger than the estimate of the  $SU(6)$

baryon-meson model (given by the central value of the red band for  $Q^2 = 0$ ), particularly for the transitions involving  $\Xi$  [see Fig. 10]. This happens because our model corrects the estimate made for the nucleon with the normalizations of the octet baryon wave functions according to Table IV. Therefore, the contributions of the valence quark core and the meson cloud are enhanced by the factor  $\sqrt{\frac{Z_{B'}}{Z_N}} \sqrt{\frac{Z_B}{Z_N}} > 1$ .

As mentioned above, the falloffs of the form factors from Figs. 8, 9 and 10 are slower than the falloff estimated for the nucleon ( $M_A \simeq 1.05$  GeV). The estimate of the falloff based on a dipole form near  $Q^2 = 1$  GeV<sup>2</sup> gives values of  $M_A$  in the range of 1.2–1.4 GeV. We conclude that the falloffs for the octet baryon  $G_A$  form factors, except for the nucleon, are consistent with the conjecture made by Gaillard and Sauvage ( $M_A = 1.25$  GeV) for the  $\Delta S = 1$  transitions [6].

### C. Results for the induced pseudoscalar form factor ( $G_P$ )

We discuss now the results for the induced pseudoscalar form factors of the octet baryons. The case of the nucleon has already been discussed in Sec. IX B. We recall that  $G_P$  has a contribution from a pseudoscalar meson pole (pion or kaon) that subsequently decays into a lepton-neutrino pair.

The reaction associated with  $\Delta I = 1$  transitions have a contribution of the pion pole (3.3), related with the  $u \leftrightarrow d$  transitions. Then, similarly to the case for the nucleon, recalling that  $M_{B'} + M_B = 2M_{BB'}$ , we use

$$G_P^{\text{pole}}(Q^2) = \frac{(M_{B'} + M_B)^2}{m_\pi^2 + Q^2} G_A^B(Q^2). \quad (10.5)$$

In the above  $G_P$  and  $G_A^B$  represent now the form factors associated with the  $B \rightarrow B'$  transition. The pole term dominates in general the  $\Delta I = 1$  transition as we will show. In addition to the pole term, there is also the contribution from the quark core due the non-zero values of the quark form factor  $g_A^q$  and  $g_P^q$ . As in the case of the nucleon, we take into account the meson cloud effect for  $G_P$  replacing the contribution from  $G_A^B$  (core contribution) by the dressed  $G_A$ , given by the replacement  $G_A^B \rightarrow \tilde{G}_A^B + G_A^{MC}$ . The expressions for the contributions  $\tilde{G}_A^B$  and  $G_A^{MC}$  have already been discussed in the previous section. Also the expressions derived for  $G_P^B$ , presented in Sec. VI, have to be corrected in the physical limit by the factor  $\sqrt{Z_{B'} Z_B}$ .

The  $\Delta S = 1$  transitions, include the transitions between the quarks  $u$  and  $s$ , are associated with a kaon pole. Therefore in the  $\Delta S = 1$  case, we replace the pion pole on the  $\Delta I = 1$  case by the kaon pole. Replacing  $m_\pi^2 \rightarrow m_K^2$  in Eq. (10.5), we obtain

$$G_P^{\text{pole}}(Q^2) = \frac{(M_{B'} + M_B)^2}{m_K^2 + Q^2} G_A^B(Q^2). \quad (10.6)$$

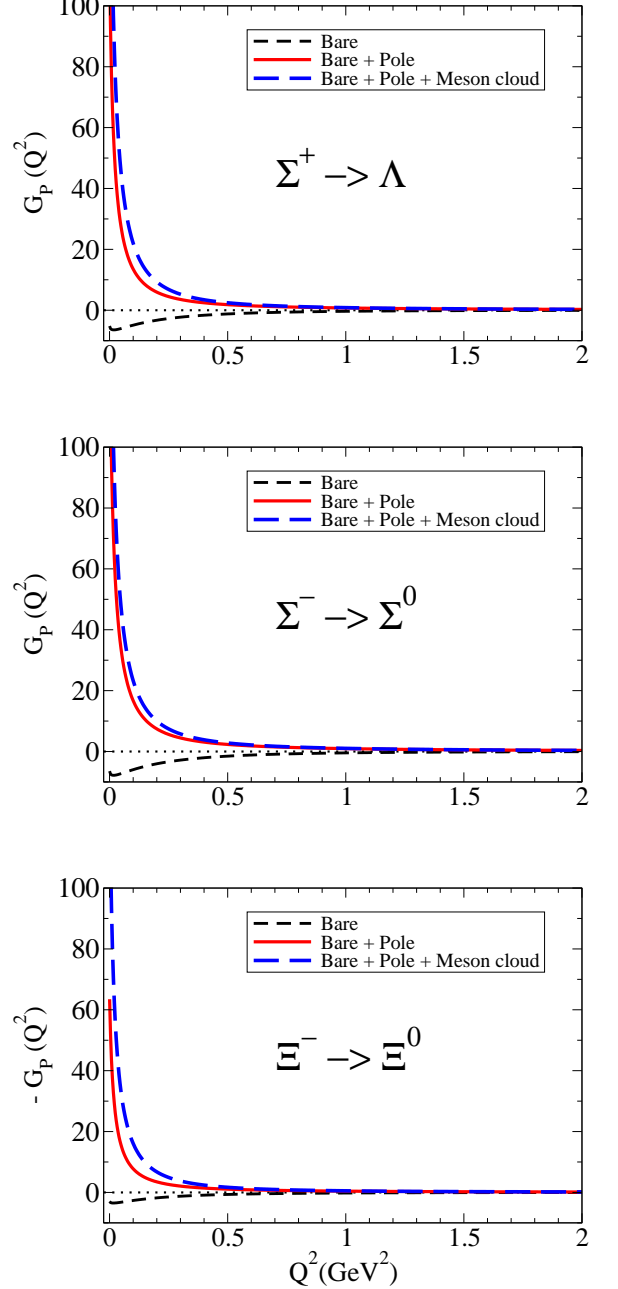


FIG. 11: Result of  $G_P(Q^2)$  for the octet baryons for  $\Delta I = 1$ . For convenience we changed the sign of the function  $G_P$  for  $\Xi^- \rightarrow \Xi^0$ .

Although it may be questionable that the pole contribution for  $G_P$  obtained for the  $\Delta I = 1$  transition (and for the nucleon) using PCAC in the chiral limit ( $m_\pi$  negligible), may be generalized for the  $\Delta S = 1$  transition, as suggested in Ref. [43], there are arguments that support this generalization. The first argument is based on the fact that lattice QCD simulations for the octet axial-vector couplings follow the generalization of the Goldberger-Treiman relation [86], which is related with Eq. (10.6) near  $Q^2 = 0$ . The second argument



			$SU(6)$		$SU'(3)$	
	$G_P^B(0)$	$G_P^{\text{pole}}(0)$	$G_P^{\text{pole}*}(0)$	$G_P(0)$	$G_P^{\text{pole}*}(0)$	$G_P(0)$
$n \rightarrow p$	-5.532	152.160	234.339	228.806	234.339	228.806
$\Sigma^+ \rightarrow \Lambda$	-5.186	118.365	182.292	177.107	193.283	188.098
$\Sigma^- \rightarrow \Sigma^0$	-6.444	144.635	118.365	216.308	202.289	195.845
$\Xi^- \rightarrow \Xi^0$	2.946	-66.420	-102.294	-99.346	-139.590	-136.643
$\Lambda \rightarrow p$	5.567	-10.771	-16.591	-11.023	-10.771	-5.203
$\Sigma^- \rightarrow n$	-1.675	4.816	3.141	3.126	6.572	4.897
$\Sigma^0 \rightarrow p$	-1.185	2.211	4.816	3.140	4.647	3.462
$\Xi^- \rightarrow \Lambda$	2.964	-5.282	-8.144	-5.180	-6.153	-3.189
$\Xi^- \rightarrow \Sigma^0$	-9.158	16.084	24.783	15.625	24.783	15.625
$\Xi^0 \rightarrow \Sigma^+$	-12.951	22.747	35.049	22.097	35.049	22.097

TABLE XI: Contributions for  $G_P$  at  $Q^2 = 0$  for the meson cloud models  $SU(6)$  and  $SU'(3)$ .  $G_P^{\text{pole}*}(0)$  represent the contribution of the meson pole term with the replacement  $G_A^B \rightarrow G_A$ .

is that the overall description given by our model for the  $G_A$  and  $G_P$  lattice data in a wide range of the pion masses ( $m_\pi = 350, \dots, 500$  MeV), motivate also the use of Eq. (10.6) for  $\Delta S = 1$ .

To obtain the “bare”, “bare + pole” and total result “bare + pole + meson cloud” for  $\Delta S = 1$ , we use the same procedure already discussed for  $\Delta I = 1$ .

The results for the case  $Q^2 = 0$  are presented in Table XI for the models  $SU(6)$  and  $SU'(3)$ . The results for the nucleon, discussed in Sec. IX B, are also included for the sake of the discussion. The differences between the two models are the consequence of the difference in the meson cloud for  $G_A(0)$ . Note the difference of results for  $G_P^{\text{pole}}(0)$  and consequently  $G_P(0)$  in the cases  $\Xi^- \rightarrow \Xi^0$  and  $\Lambda \rightarrow p$ . The effect of the kaon pole for the  $\Lambda \rightarrow p$  transition ( $\Delta S = 1$ ) is much smaller than the pion pole for the  $\Xi^- \rightarrow \Xi^0$  transition ( $\Delta I = 1$ ). The physical pion is closer to the chiral limit than the kaon.

Results for  $G_P$  by the  $SU'(3)$  meson cloud model related with  $\Delta I = 1$  transitions are presented in Fig. 11, while those related with  $\Delta S = 1$  transitions are presented in Figs. 12 and 13. The results associated with the  $SU(6)$  meson cloud model are similar in shape, but differ in values for small  $Q^2$ .

In Fig. 11 we can observe the dominance of the pole term for the  $\Delta I = 1$  transitions, since the values of “bare + pole” are much larger in absolute value than the values of “bare”. All the results are very similar although the magnitude of the pole contribution is small for the  $\Xi^- \rightarrow \Xi^0$  case, because the magnitude of  $G_A$  is also small in this transition. The similarity is a consequence of the approximated  $SU(6)$  structure of  $G_A^B$  and  $G_P^B$  that results from the quark model and the small  $SU(6)$  violation from the meson cloud component.

In Figs. 12 and 13 we can notice that the magnitude of  $G_P$  for the transitions  $\Delta S = 1$  is smaller than that for the case of the  $\Delta I = 1$  transitions. In this case the contributions from the pole are reduced by about an order

of magnitude, due to the difference in the meson masses, that contributes with a reduction of about  $\frac{m_K^2}{m_\pi^2} \simeq 12.9$ , corrected by the factors  $M_{BB'}^2$ , depending on the transition [see Eqs. (10.5) and (10.6)].

Thus, in the  $\Delta S = 1$  transitions the bare and pole contributions are comparable in magnitude, and the dominance of the pole term does not happen as in the case  $\Delta I = 1$ . In Fig. 12 for the transitions  $\Lambda \rightarrow p$ ,  $\Sigma^- \rightarrow n$  and  $\Sigma^0 \rightarrow p$ , we can observe a significant cancellation between the bare and pole contributions. The evidence of the cancellation can be observed due to the small values of “bare + pole” when compared with “bare” in absolute values. The calculation is more significant for the  $\Sigma^0 \rightarrow p$  transition. One can see however, that when  $Q^2$  increases the pole contribution dominates (positive values for  $G_P$  or  $-G_P$  according to the transition). This happens because although the bare contributions goes with  $1/Q^4$  as discussed in Sec. VI, while the pole goes with  $1/Q^6$  for very large  $Q^2$ , the factor  $1/(m_K^2 + Q^2)$  in the pole term dominates over the other terms in the region observed ( $Q^2 < 2$  GeV<sup>2</sup>). Since  $m_K^2 \simeq 0.25$  GeV<sup>2</sup>, the factor  $1/(m_K^2 + Q^2)$  has a strong impact for the small and the intermediate  $Q^2$  regions. For much larger  $Q^2$  the bare contribution will dominate.

The results for the transitions involving  $\Xi$  presented in Fig. 13 are very similar, apart the scale. In the case of the  $\Xi^- \rightarrow \Sigma^0$  and  $\Xi^0 \rightarrow \Sigma^+$  transitions the similarity is a consequence of  $SU(3)$  symmetry for  $G_A$ , since they differ only by the factor  $1/\sqrt{2}$ , and the masses are the same in both transitions. As for  $\Xi^- \rightarrow \Lambda$ , this is a consequence of the approximated  $SU(6)$  structure which implies a reduction of the pole contribution of the factor  $\frac{5}{\sqrt{3}} \simeq 3$  compared to  $\Xi^- \rightarrow \Sigma^0$ , neglecting the effect of the (small) mass difference between the  $\Sigma$  and  $\Lambda$ .

Our result for the  $G_P$  (full result) associated with  $\Xi^0 \rightarrow \Sigma^+$  transition has a magnitude similar to that of the lattice QCD results in Ref. [78].

To finalize, it is interesting to discuss the breaking of

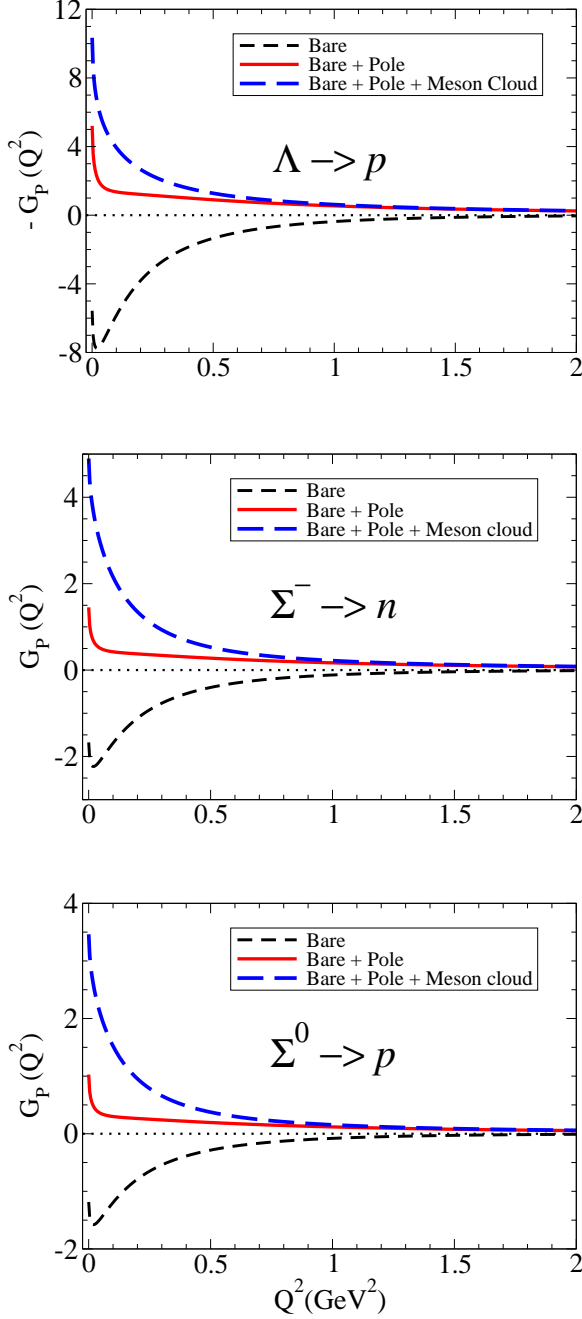


FIG. 12: Results of  $G_P(Q^2)$  for the octet baryons for  $\Delta S = 1$  (part 1). For convenience we changed the sign of the function  $G_P$  for  $\Lambda \rightarrow p$ .

$SU(3)$  symmetry due to the difference in the transitions between  $\Delta I = 1$  and  $\Delta S = 1$ . This can be observed by comparing the transitions  $n \rightarrow p$  and  $\Xi^0 \rightarrow \Sigma^+$ , which, according to the  $SU(3)$  baryon-meson model, have the same results for the axial-vector form factor at  $Q^2 = 0$ ,  $G_A(0) = F + D$ . However, since the value of  $G_P(0)$  for the pole is determined by the pion mass (squared) for the reaction with  $\Delta I = 1$  and by the kaon mass (squared) for

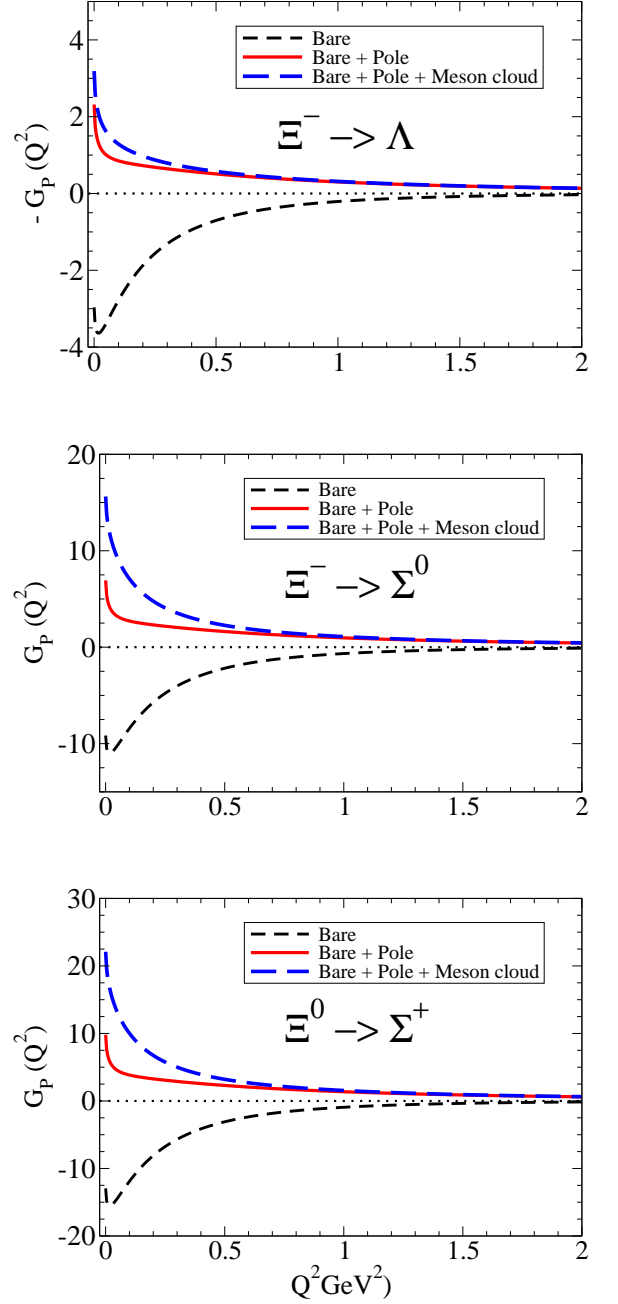


FIG. 13: Results of  $G_P(Q^2)$  for the octet baryons for  $\Delta S = 1$  (part 2). For convenience we changed the sign of the function  $G_P$  for  $\Xi^- \rightarrow \Lambda$ .

the reaction with  $\Delta S = 1$ , the magnitude of the  $G_P^{\text{pole}}(0)$  changes drastically from the  $\Delta I = 1$  to  $\Delta S = 1$  cases. From Table XI we can conclude that the ratio between the pole terms for the nucleon and  $\Xi^0 \rightarrow \Sigma^+$  is about 6.7, which is essentially the result of the combination of the baryon and meson masses,  $\frac{M^2}{M_{BB'}^2} \frac{m_\pi^2}{m_K^2} \simeq 7.2$ , where  $M_{BB'}$  is the average mass of the initial and final baryons in the  $\Xi$  transitions. The value 7.2 has to be corrected

by a factor 7% due to the difference in the values of  $G_A(0)$  which correspond to the deviation from the  $SU(6)$  baryon-meson model. We can conclude then, that the pole term (pion or kaon) breaks the  $SU(3)$  symmetry for  $G_P$ , but that the magnitude of the breaking is mainly a consequence of the ratio  $\frac{m_\pi^2}{m_K^2}$ .

## XI. SUMMARY AND CONCLUSIONS

Weak interaction axial form factors of the octet baryons have been studied extensively based on a large numbers of theoretical frameworks. However, such studies have mostly been restricted to the axial charges and properties at  $Q^2 = 0$ . In this work we use the covariant spectator quark model to probe the weak interaction axial structure of the octet baryons and take advantage of the covariance to make predictions on the  $Q^2$  dependence of the axial form factors  $G_A(Q^2)$  and  $G_P(Q^2)$ , for all the octet baryon weak interaction axial transitions.

In the covariant spectator quark model the quarks have their own structure characterized by the electromagnetic and axial form factors, that can be used to calculate electromagnetic and weak interaction transition form factors between baryons. The model has been successfully used in the past for the studies of several electromagnetic transitions between baryons, including in particular the electromagnetic structure of the nucleon, the octet and decuplet baryons, and other reactions. In the future the present approach can be applied for the weak interaction vector transition form factors, replacing the quark axial current  $j_{Aq}^\mu$  by the quark electromagnetic-vector current. Similar calculations were already performed for the octet baryon electromagnetic form factors using an  $S$ -state model [106, 109, 111, 112], except that it is necessary now to consider also charged currents.

To study the weak interaction axial structure of the octet baryons the covariant spectator quark model is first calibrated by the lattice QCD and the physical data for nucleon. After that, the model is extended for the octet baryons using the  $SU_F(3)$  (flavor) symmetry. The  $SU_F(3)$  symmetry breaking effects are taken into account by the octet baryon masses and the shape of the radial wave functions, determined in previous works by the study of the electromagnetic properties in the context of the covariant spectator quark model. For simplicity we neglected the difference in the masses of the initial and the final baryons. The axial form factors are then calculated in the relativistic impulse approximation in terms of the covariant wave functions of the octet baryons and the quark axial current, defined by the quark axial form factors  $g_A^q(Q^2)$  and  $g_P^q(Q^2)$ . The wave functions of the octet baryons are determined by a dominant  $S$ -state component defined in previous works, and a  $P$ -state is introduced in this work, in order to better describe the axial-vector form factors of the octet baryons. The addition of the extra  $P$ -state was suggested by some studies based on the quark degrees of freedom.

The calibration of the present model is done as follows: the quark form factor  $g_A^q(Q^2)$  is assumed to have the same form as that of the quark electromagnetic isovector form factor  $f_{1-}(Q^2)$ , and the quark form factor  $g_P^q(Q^2)$  has a form analogous to the Pauli form factors of the quarks, motivated by vector meson dominance with two adjustable parameters. The unknown parameters of the model are, the  $P$ -state mixture coefficient, and the parameters of the  $g_P^q(Q^2)$  function, and they are determined by a fit to the nucleon axial form factor data in the lattice QCD regime. In this regime the contamination of the form factors due to the meson cloud is significantly suppressed and the physics associated with the valence quarks can be estimated more accurately.

The results obtained for the octet baryon  $G_A$  form factors are consistent with the nonrelativistic  $SU(6)$  quark models in the equal mass case ( $M_B = M$ ) when the  $P$ -state component is dropped ( $n_P = 0$ ). In addition, the model at  $Q^2 = 0$  has the same structure of an  $SU(6)$  quark model or an  $SU(6)$  baryon-meson model, even when the  $P$ -state is included.

We conclude that the axial form factors of the nucleon, both  $G_A$  and  $G_P$ , can be very well explained in the lattice regime of our constituent quark model with a  $P$ -state mixture of about 26%. Once the parameters of the model are fixed, the results can be extrapolated to the physical regime and used to calculate the contributions of the valence quarks for the nucleon axial form factors. As in previous works on the nucleon axial-vector form factor, we conclude also that only the effects of the valence quarks underestimate the  $G_A$  data in the physical regime. Under the assumption that the missing part is due to the meson cloud component in the physical nucleon state, we used the model, which is well calibrated in the high  $Q^2$  region, to estimate the size of the meson cloud contribution in the physical nucleon state. The results obtained for the nucleon are in agreement with the experimental data for  $G_A$  and  $G_P$ , when the fraction of the meson cloud in the nucleon wave function is about 27%. With the use of the lattice QCD and physical data for the axial form factors, we obtain in principle a better constraint for the magnitude of the meson cloud than when we use only the constraint of the nucleon electromagnetic form factor data.

Using the  $SU_F(3)$  symmetry at the quark level we generalize the model for the octet baryons, and predict all the axial form factors of the octet baryons. It is expected that the present estimates is accurate for  $Q^2 > 1 \text{ GeV}^2$  (large  $Q^2$  regime) except for a small correction due to the normalization factor of baryon the wave functions, that result from the meson cloud component. The corrections are estimated based on the relation for the meson cloud in the nucleon wave function and the other members of the octet baryon wave functions. As for the low  $Q^2$  regime ( $Q^2 < 1 \text{ GeV}^2$ ), the estimates based exclusively on the valence quark degrees of freedom are expected to fail. We provide however, effective descriptions for the region  $Q^2 < 1 \text{ GeV}^2$ , based on simple parametrizations for the

meson cloud contributions constrained by  $SU(3)$  and/or  $SU(6)$  symmetries. Those parametrizations can be useful in the future for the studies associated with the properties of octet baryons. The meson cloud model labeled as  $SU'(3)$ , gives the best description of the data within an deviation of three standard deviations.

We conclude in general, that the naive  $SU(6)$  baryon-meson model is expected to fail at large  $Q^2$  for the  $\Delta I = 1$  transitions. In this case the falloff observed for the nucleon given by the cutoff parameter  $M_A \simeq 1.05$  GeV in the dipole parametrization, should be replaced by a value near 1.25 GeV. As for the transitions  $\Delta S = 1$ , although dependent on the transitions, are consistent with the estimate  $M_A \simeq 1.25$  GeV, proposed long time ago [6]. Predictions for the induced pseudoscalar form factors are also presented in this work based on the contribution of the meson pole (pion for  $\Delta I = 1$  and kaon for  $\Delta S = 1$  transitions), complemented by a contribution from the bare core. The bare contribution used in this work is derived from the quark substructure of the baryons, and it is calibrated using lattice QCD data. As far as the authors are aware, this is the first time that the  $G_P$  form factors with finite  $Q^2$  are estimated using the results from lattice QCD as input.

To summarize, we present the result of a phenomenological fit with some constraints based on a constituent quark model combined with a parametrization of meson cloud effects for the octet baryon weak interaction form factors  $G_A(Q^2)$  and  $G_P(Q^2)$ . The model presented is covariant and can therefore be used for the studies of the reactions at large  $Q^2$ . The predictions of the model, in particular the falloff of the  $G_A(Q^2)$ , can be tested in the near future by lattice QCD simulations, or hopefully by upcoming experiments.

### Acknowledgments

The authors thank P. Guichon for sharing the data for  $G_P$ . GR thanks Alireza Tavanfar for his comments and suggestions. GR was supported by the Brazilian Ministry of Science, Technology and Innovation (MCTI-Brazil). KT was also supported by FAPESP, 2014/26892-8. GR and KT were also supported by Conselho Nacional de Desenvolvimento Científico e Tecnológico (CNPq) 400826/2014-3.

### Appendix A: Calculation of the transition currents

We discuss here how we calculate the factors associated with radial wave functions using the symmetries of the functions.

First, we present identities that can be used in the calculation of transitions between the states of the same mass. Next, we discuss the angular integration that can be used to simplify the calculations for the nucleon, including the terms associated with the same state ( $S$  or

$P$ ) as well as the terms associated with the  $S$  and  $P$  mixture (different states). Finally, we explain how the procedure can be extended for transitions between the different baryon states which requires also different parametrizations between the initial and the final states.

#### 1. Integral identities

The following relations are valid under the integration symbol when the radial wave functions of the initial and final state are defined for the states with the same mass:

$$k^\alpha = \frac{P' \cdot k}{(P')^2} (P')^\alpha \quad (\text{A1})$$

$$k^\alpha k^\beta = S_1 g^{\alpha\beta} + \frac{m_D^2 + S_2}{(P')^2} (P')^\alpha (P')^\beta + \frac{S_3}{Q^2} q^\alpha q^\beta \quad (\text{A2})$$

$$(k \cdot q) k^\alpha = -c_2 q^\alpha, \quad (\text{A3})$$

where  $\sqrt{P'^2} = M(1 + \tau)$  and  $S_1 = \frac{1}{2}(c_2 - c_1)$ ,  $S_2 = -\frac{1}{2}(c_2 - 3c_1)$  and  $S_3 = \frac{1}{2}(3c_2 - c_1)$ .

#### 2. Angular integration – nucleon case

The expression for the transition currents depends on a few covariant integrals. The integrals are by definition frame independent, however, the symmetries of the radial wave functions are better understood by fixing a frame. We consider in particular the Breit frame. In the Breit frame  $P' = (M\sqrt{1 + \tau}, 0, 0, 0)$  and  $q = (0, 0, 0, Q)$ . In this reference frame we can represent the initial radial wave function  $\psi_i(P_-, k)$  as a function of  $\omega_- = \frac{P_+ \cdot k}{M} = a + bk_z$  and the final radial wave function  $\psi_f(P_+, k)$  as a function of  $\omega_+ = \frac{P_+ \cdot k}{M} = a - bk_z$ . Here  $a$  and  $b$  are functions of  $\mathbf{k}$  and independent of the angles.<sup>2</sup> When the initial and the final states are the same ( $i = f$ ) as in the case of the transition between  $S$  states or  $P$  states, we can conclude right away that the product of the wave functions becomes

$$\psi_i(P_+, k) \psi_i(P_-, k) = F(z), \quad (\text{A4})$$

where  $F$  is an implicit function of  $|\mathbf{k}|$ , and  $z = k_z/|\mathbf{k}|$  represents  $\cos\theta$  ( $\theta$ , the angle between  $\mathbf{k}$  and the  $z$ -axis). Since the integration range in  $z$  is bounded by the  $-1$  and  $+1$ , one can conclude that

$$\int_k k_z \psi_i(P_+, k) \psi_i(P_-, k) = 0. \quad (\text{A5})$$

<sup>2</sup> The explicit expressions are

$$a = \frac{P' \cdot k}{M}, \quad bk_z = -\frac{q \cdot k}{M}.$$

In the Breit frame  $a = \sqrt{1 + \tau} E_D$  and  $b = \frac{Q}{2M}$ .



Therefore, the terms proportional to  $k_z$  vanishes in the integration. The same happens trivially for the terms proportional to  $k_x$  or  $k_y$ .

In the case of the transition between the S and the P states one can have terms in  $\psi_P(P_+, k)\psi_S(P_-, k) = F(z)$ , and  $\psi_S(P_+, k)\psi_P(P_-, k) = F(-z)$ , where the argument  $z$  changes sign from the  $S \rightarrow P$  to the  $P \rightarrow S$  cases. In this case we have to combine the contributions from the both processes which can take the form  $t_1 F(z) + t_2 F(-z)$ , where  $t_1, t_2$  are independent of  $z$ . We note that one can change  $-z \rightarrow z$  in the second term, under the integration symbol, since

$$\int_{-1}^1 F(z) dz = \int_{-1}^1 F(-z) dz. \quad (\text{A6})$$

Using the same argument one can conclude also that

$$\int_{-1}^1 z F(z) dz = 0. \quad (\text{A7})$$

Therefore, the terms in  $k_z$  vanishes also in the integral appearing in the  $S - P$  transition,

$$\int_k k_z \psi_f(P_+, k) \psi_i(P_-, k) = 0, \quad (\text{A8})$$

and the same holds for the change of the initial and final state interchange,  $i \leftrightarrow f$ .

### 3. Angular integration – octet case

The calculation of integrals associated with the transitions between the different states, which involves different parametrizations of the radial wave functions, can be reduced to the case discussed in the previous section for the nucleon, provided that the radial wave functions are associated with the same mass.

In the equal mass case the discussion associated with the  $S$ - and  $P$ -states can be generalized for radial wave functions with different parametrizations for the initial and final states. The key point again is that we can re-write the factors associated with the radial wave functions in terms of the  $\omega_+$  and  $\omega_-$  as already discussed.

- 
- [1] I. G. Aznauryan, A. Bashir, V. Braun, S. J. Brodsky, V. D. Burkert, L. Chang, C. Chen and B. El-Bennich *et al.*, *Int. J. Mod. Phys. E*, Vol. 22, **1330015** (2013) [arXiv:1212.4891 [nucl-th]].
- [2] V. Bernard, L. Elouadrhiri and U. G. Meissner, *J. Phys. G* **28**, R1 (2002) [hep-ph/0107088].
- [3] E. J. Beise, *Eur. Phys. J. A* **24S2**, 43 (2005) [nucl-ex/0501019].
- [4] T. Gorringer and H. W. Fearing, *Rev. Mod. Phys.* **76**, 31 (2004) [nucl-th/0206039].
- [5] M. R. Schindler and S. Scherer, *Eur. Phys. J. A* **32**, 429 (2007) [hep-ph/0608325].
- [6] J. M. Gaillard and G. Sauvage, *Ann. Rev. Nucl. Part. Sci.* **34**, 351 (1984).
- [7] V. Bernard, *Prog. Part. Nucl. Phys.* **60**, 82 (2008) [arXiv:0706.0312 [hep-ph]].
- [8] A. Airapetian *et al.* [HERMES Collaboration], *Phys. Rev. D* **75**, 012007 (2007) [hep-ex/0609039].
- [9] F. Gross, G. Ramalho and M. T. Peña, *Phys. Rev. D* **85**, 093006 (2012) [arXiv:1201.6337 [hep-ph]].
- [10] F. Myhrer and A. W. Thomas, *Phys. Lett. B* **663**, 302 (2008) [arXiv:0709.4067 [hep-ph]].
- [11] P. E. Shanahan, A. W. Thomas, K. Tsushima, R. D. Young and F. Myhrer, *Phys. Rev. Lett.* **110**, 202001 (2013) [arXiv:1302.6300 [nucl-th]].
- [12] N. Isgur, *Phys. Rev. D* **59**, 034013 (1999) [hep-ph/9809255].
- [13] D. Barquilla-Cano, A. J. Buchmann and E. Hernandez, *Eur. Phys. J. A* **27**, 365 (2006) [hep-ph/0611248].
- [14] D. Drakoulakos *et al.* [MINERvA Collaboration], hep-ex/0405002.
- [15] Y. Itow *et al.* [T2K Collaboration], hep-ex/0106019.
- [16] C. Anderson *et al.* [ArgoNeuT Collaboration], *JINST* **7**, P10020 (2012) [arXiv:1205.6702 [physics.ins-det]].
- [17] S. X. Nakamura, H. Kamano and T. Sato, *Phys. Rev. D* **92**, 074024 (2015) [arXiv:1506.03403 [hep-ph]].
- [18] M. R. Alam, M. S. Athar, S. Chauhan and S. K. Singh, arXiv:1509.08622 [hep-ph].
- [19] T. Sato, D. Uno and T. S. H. Lee, *Phys. Rev. C* **67**, 065201 (2003) [nucl-th/0303050].
- [20] S. M. Bilenky and E. Christova, *Phys. Part. Nucl. Lett.* **10**, 651 (2013) [arXiv:1307.7275].
- [21] G. Bardin, J. Duclos, A. Magnon, J. Martino, A. Richter, E. Zavattini, A. Bertin and M. Piccinini *et al.*, *Phys. Lett. B* **104**, 320 (1981).
- [22] S. Choi, V. Estenne, G. Bardin, N. De Botton, G. Fournier, P. A. M. Guichon, C. Marchand and J. Marroncle *et al.*, *Phys. Rev. Lett.* **71**, 3927 (1993).
- [23] V. A. Andreev *et al.* [MuCap Collaboration], *Phys. Rev. Lett.* **99**, 032002 (2007) [arXiv:0704.2072 [nucl-ex]].
- [24] K. A. Olive *et al.* [Particle Data Group Collaboration], *Chin. Phys. C* **38**, 090001 (2014).
- [25] S. L. Glashow, *Physica A* **96**, 27 (1979).
- [26] J. F. Donoghue, B. R. Holstein and S. W. Klimt, *Phys. Rev. D* **35**, 934 (1987).
- [27] J. F. Donoghue, E. Golowich, and B. R. Holstein, *Dynamics of the Standard Model*, Cambridge Monographs on Particle Physics, Nuclear Physics and Cosmology, Vol. 2 (University Press, Cambridge, 1994)
- [28] F. Schlumpf, *Phys. Rev. D* **47**, 4114 (1993) [*Phys. Rev. D* **49**, 6246 (1994)] [hep-ph/9212250].
- [29] G. Hellstern, R. Alkofer, M. Oettel and H. Reinhardt, *Nucl. Phys. A* **627**, 679 (1997) [hep-ph/9705267].
- [30] L. Y. Glozman, M. Radici, R. F. Wagenbrunn, S. Boffi, W. Klink and W. Plessas, *Phys. Lett. B* **516**, 183 (2001) [nucl-th/0105028].
- [31] S. Boffi, L. Y. Glozman, W. Klink, W. Plessas, M. Radici and R. F. Wagenbrunn, *Eur. Phys. J. A* **14**, 17 (2002) [hep-ph/0108271].
- [32] J. Franklin, *Phys. Rev. D* **66**, 033010 (2002).
- [33] D. Merten, U. Loring, K. Kretzschmar, B. Metsch and H. R. Petry, *Eur. Phys. J. A* **14**, 477 (2002) [hep-ph/0204024].
- [34] B. Julia-Diaz, D. O. Riska and F. Coester, *Phys. Rev. C* **69**, 035212 (2004) [Erratum-ibid. *C* **75**, 069902 (2007)] [hep-ph/0312169]; B. Julia-Diaz, D. O. Riska and F. Coester, *Phys. Rev. C* **70**, 045204 (2004) [nucl-th/0406015].
- [35] D. Barquilla-Cano, A. J. Buchmann and E. Hernandez, *Nucl. Phys. A* **714**, 611 (2003) [nucl-th/0204067].
- [36] K. S. Choi, W. Plessas and R. F. Wagenbrunn, *Phys. Rev. D* **82**, 014007 (2010) [arXiv:1005.0337 [hep-ph]].
- [37] B. A. Li, arXiv:1411.6029 [hep-ph].
- [38] G. Eichmann and C. S. Fischer, *Eur. Phys. J. A* **48**, 9 (2012) [arXiv:1111.2614 [hep-ph]].
- [39] L. Chang, C. D. Roberts and S. M. Schmidt, *Phys. Rev. C* **87**, 015203 (2013) [arXiv:1207.5300 [nucl-th]].
- [40] S. X. Qin, C. D. Roberts and S. M. Schmidt, *Phys. Lett. B* **733**, 202 (2014) [arXiv:1402.1176 [nucl-th]].
- [41] N. Yamanaka, S. Imai, T. M. Doi and H. Suganuma, *Phys. Rev. D* **89**, 074017 (2014) [arXiv:1401.2852 [hep-ph]].
- [42] A. W. Thomas, *Adv. Nucl. Phys.* **13**, 1 (1984); S. Theberge and A. W. Thomas, *Nucl. Phys. A* **393**, 252 (1983).
- [43] K. Kubodera, Y. Kohyama, K. Oikawa and C. W. Kim, *Nucl. Phys. A* **439**, 695 (1985); K. Tsushima, T. Yamaguchi, Y. Kohyama and K. Kubodera, *Nucl. Phys. A* **489**, 557 (1988). K. Tsushima, T. Yamaguchi, M. Takizawa, Y. Kohyama and K. Kubodera, *Phys. Lett. B* **205**, 128 (1988).
- [44] T. Yamaguchi, K. Tsushima, Y. Kohyama and K. Kubodera, *Nucl. Phys. A* **500**, 429 (1989); Y. Kohyama, K. Oikawa, K. Tsushima and K. Kubodera, *Phys. Lett. B* **186**, 255 (1987).
- [45] H. Hogaasen and F. Myhrer, *Phys. Rev. D* **37**, 1950 (1988).
- [46] K. Khosonhongkee, V. E. Lyubovitskij, T. Gutsche, A. Faessler, K. Pumsaard, S. Cheedket and Y. Yan, *J. Phys. G* **30**, 793 (2004) [hep-ph/0403119].
- [47] B. Pasquini and S. Boffi, *Phys. Rev. D* **76**, 074011 (2007) [arXiv:0707.2897 [hep-ph]].
- [48] A. Silva, H. C. Kim, D. Urbano and K. Goeke, *Phys. Rev. D* **72**, 094011 (2005) [hep-ph/0509281].
- [49] T. Ledwig, A. Silva, H. C. Kim and K. Goeke, *JHEP* **0807**, 132 (2008) [arXiv:0806.4072 [hep-ph]].
- [50] C. Lorce, *Phys. Rev. D* **78**, 034001 (2008) [arXiv:0708.3139 [hep-ph]].
- [51] C. Adamuscin, E. Tomasi-Gustafsson, E. Santopinto and R. Bijker, *Phys. Rev. C* **78**, 035201 (2008) [arXiv:0706.3509 [nucl-th]].
- [52] X. Y. Liu, K. Khosonhongkee, A. Limphirat, P. Sue-

- bka and Y. Yan, Phys. Rev. D **91**, 034022 (2015) [arXiv:1406.7633 [hep-ph]].
- [53] H. Dahiya and M. Randhawa, Phys. Rev. D **90**, 074001 (2014) [arXiv:1409.4943 [hep-ph]].
- [54] G. S. Yang and H. C. Kim, Phys. Rev. C **92**, 035206 (2015) [arXiv:1504.04453 [hep-ph]].
- [55] V. Bernard, N. Kaiser and U. G. Meissner, Phys. Rev. D **50**, 6899 (1994) [hep-ph/9403351].
- [56] J. J. de Swart, Rev. Mod. Phys. **35**, 916 (1963) [Rev. Mod. Phys. **37**, 326 (1965)].
- [57] E. E. Jenkins and A. V. Manohar, Phys. Lett. B **255**, 558 (1991); E. E. Jenkins and A. V. Manohar, Phys. Lett. B **259**, 353 (1991)
- [58] J. Dai, R. F. Dashen, E. E. Jenkins and A. V. Manohar, Phys. Rev. D **53**, 273 (1996) [hep-ph/9506273].
- [59] M. J. Savage and J. Walden, Phys. Rev. D **55**, 5376 (1997) [hep-ph/9611210].
- [60] R. Flores-Mendieta, E. E. Jenkins and A. V. Manohar, Phys. Rev. D **58**, 094028 (1998) [hep-ph/9805416].
- [61] M. R. Schindler, T. Fuchs, J. Gegelia and S. Scherer, Phys. Rev. C **75**, 025202 (2007) [nucl-th/0611083].
- [62] M. Procura, B. U. Musch, T. R. Hemmert and W. Weise, Phys. Rev. D **75**, 014503 (2007) [hep-lat/0610105].
- [63] M. E. Carrillo-Serrano, I. C. Cloët and A. W. Thomas, Phys. Rev. C **90**, 064316 (2014) [arXiv:1409.1653 [nucl-th]].
- [64] T. Ledwig, J. Martin Camalich, L. S. Geng and M. J. Vicente Vacas, Phys. Rev. D **90**, 054502 (2014) [arXiv:1405.5456 [hep-ph]].
- [65] B. C. Tiburzi, Phys. Rev. D **91**, 094510 (2015) [arXiv:1503.06329 [hep-lat]].
- [66] E. M. Henley, W. Y. P. Hwang and L. S. Kisslinger, Phys. Rev. D **46**, 431 (1992).
- [67] Z. -G. Wang, S. -L. Wan and W. -M. Yang, Eur. Phys. J. C **47**, 375 (2006) [hep-ph/0601060].
- [68] G. Erkol and A. Ozpineci, Phys. Rev. D **83**, 114022 (2011) [arXiv:1105.1637 [hep-ph]].
- [69] S. Sasaki *et al.* [RIKEN-BNL-Columbia-KEK Collaboration], Phys. Rev. D **68**, 054509 (2003) [hep-lat/0306007].
- [70] R. G. Edwards *et al.* [LHPC Collaboration], Phys. Rev. Lett. **96**, 052001 (2006) [hep-lat/0510062].
- [71] R. Horsley, Y. Nakamura, A. Nobile, P. E. L. Rakow, G. Schierholz and J. M. Zanotti, Phys. Lett. B **732**, 41 (2014) [arXiv:1302.2233 [hep-lat]].
- [72] T. Bhattacharya, S. D. Cohen, R. Gupta, A. Joseph, H. W. Lin and B. Yoon, Phys. Rev. D **89**, 094502 (2014) [arXiv:1306.5435 [hep-lat]].
- [73] T. Yamazaki *et al.* [RBC+UKQCD Collaboration], Phys. Rev. Lett. **100**, 171602 (2008) [arXiv:0801.4016 [hep-lat]].
- [74] J. R. Green, M. Engelhardt, S. Krieg, J. W. Negele, A. V. Pochinsky and S. N. Syritsyn, Phys. Lett. B **734**, 290 (2014) [arXiv:1209.1687 [hep-lat]].
- [75] A. Abdel-Rehim *et al.*, Phys. Rev. D **92**, 114513 (2015) [arXiv:1507.04936 [hep-lat]].
- [76] G. S. Bali *et al.*, Phys. Rev. D **91**, 054501 (2015) [arXiv:1412.7336 [hep-lat]].
- [77] K. F. Liu, S. J. Dong, T. Draper, J. M. Wu and W. Wilcox, Phys. Rev. D **49**, 4755 (1994) [hep-lat/9305025].
- [78] S. Sasaki and T. Yamazaki, Phys. Rev. D **78**, 014510 (2008) [arXiv:0709.3150 [hep-lat]].
- [79] T. Yamazaki, Y. Aoki, T. Blum, H. -W. Lin, S. Ohta, S. Sasaki, R. Tweedie and J. Zanotti, Phys. Rev. D **79**, 114505 (2009) [arXiv:0904.2039 [hep-lat]].
- [80] J. D. Bratt *et al.* [LHPC Collaboration], Phys. Rev. D **82**, 094502 (2010) [arXiv:1001.3620 [hep-lat]].
- [81] C. Alexandrou, M. Constantinou, S. Dinter, V. Drach, K. Jansen, C. Kallidonis and G. Koutsou, Phys. Rev. D **88**, 014509 (2013) [arXiv:1303.5979 [hep-lat]].
- [82] C. Alexandrou *et al.* [ETM Collaboration], Phys. Rev. D **83**, 045010 (2011) [arXiv:1012.0857 [hep-lat]].
- [83] A. Abdel-Rehim, C. Alexandrou, M. Constantinou, V. Drach, K. Hadjiyiannakou, K. Jansen, G. Koutsou and A. Vaquero, Phys. Rev. D **89**, 034501 (2014) [arXiv:1310.6339 [hep-lat]].
- [84] S. Sasaki and T. Yamazaki, Phys. Rev. D **79**, 074508 (2009) [arXiv:0811.1406 [hep-ph]].
- [85] H. -W. Lin and K. Orginos, Phys. Rev. D **79**, 034507 (2009) [arXiv:0712.1214 [hep-lat]].
- [86] G. Erkol, M. Oka and T. T. Takahashi, Phys. Lett. B **686**, 36 (2010) [arXiv:0911.2447 [hep-lat]].
- [87] C. Alexandrou, M. Constantinou, K. Hadjiyiannakou, K. Jansen, C. Kallidonis and G. Koutsou, arXiv:1411.3494 [hep-lat].
- [88] J. D. Sullivan, Phys. Rev. D **5**, 1732 (1972).
- [89] A. W. Thomas, Phys. Lett. B **126**, 97 (1983).
- [90] E. M. Henley and G. A. Miller, Phys. Lett. B **251**, 453 (1990).
- [91] S. Kumano, Phys. Rev. D **43**, 59 (1991); S. Kumano, Phys. Rev. D **43**, 3067 (1991); S. Kumano and J. T. Londergan, Phys. Rev. D **44**, 717 (1991).
- [92] S. M. Bilenky and E. Christova, J. Phys. G **40**, 075004 (2013) [arXiv:1303.3710 [hep-ph]].
- [93] A. V. Butkevich and D. Perevalov, Phys. Rev. D **89**, 053014 (2014) [arXiv:1311.3754 [hep-ph]].
- [94] J. E. Amaro and E. R. Arriola, arXiv:1510.07532 [nucl-th].
- [95] B. Bhattacharya, G. Paz and A. J. Troviano, Phys. Rev. D **92**, 113011 (2015) [arXiv:1510.05652 [hep-ph]].
- [96] M. J. Musolf, T. W. Donnelly, J. Dubach, S. J. Pollock, S. Kowalski and E. J. Beise, Phys. Rept. **239**, 1 (1994).
- [97] K. Tsushima, H. C. Kim and K. Saito, Phys. Rev. C **70**, 038501 (2004) [nucl-th/0307013]; M. K. Cheoun, K. Choi, K. S. Kim, K. Saito, T. Kajino, K. Tsushima and T. Maruyama, Phys. Lett. B **723**, 464 (2013) [arXiv:1302.5770 [nucl-th]]; M. K. Cheoun, K. S. Choi, K. S. Kim, K. Saito, T. Kajino, K. Tsushima and T. Maruyama, Phys. Rev. C **87**, 065502 (2013) [arXiv:1303.5920 [nucl-th]].
- [98] F. Gross, G. Ramalho and M. T. Peña, Phys. Rev. C **77**, 015202 (2008) [nucl-th/0606029].
- [99] F. Gross, G. Ramalho and M. T. Peña, Phys. Rev. D **85**, 093005 (2012) [arXiv:1201.6336 [hep-ph]].
- [100] F. Gross, G. Ramalho and M. T. Peña, Phys. Rev. C **77**, 035203 (2008).
- [101] G. Ramalho, M. T. Peña and F. Gross, Eur. Phys. J. A **36**, 329 (2008) [arXiv:0803.3034 [hep-ph]]; G. Ramalho, M. T. Peña and F. Gross, Phys. Rev. D **78**, 114017 (2008) [arXiv:0810.4126 [hep-ph]].
- [102] G. Ramalho and M. T. Peña, J. Phys. G **36**, 115011 (2009) [arXiv:0812.0187 [hep-ph]].
- [103] G. Ramalho and M. T. Peña, Phys. Rev. D **80**, 013008 (2009) [arXiv:0901.4310 [hep-ph]].
- [104] G. Ramalho and K. Tsushima, Phys. Rev. D **81**, 074020 (2010) [arXiv:1002.3386 [hep-ph]].

- [105] G. Ramalho, Phys. Rev. D **90**, 033010 (2014) [arXiv:1407.0649 [hep-ph]]; G. Ramalho and K. Tsushima, Phys. Rev. D **89**, 073010 (2014) [arXiv:1402.3234 [hep-ph]]; G. Ramalho and M. T. Peña, Phys. Rev. D **89**, 094016 (2014) [arXiv:1309.0730 [hep-ph]]; G. Ramalho and M. T. Peña, Phys. Rev. D **84**, 033007 (2011) [arXiv:1105.2223 [hep-ph]].
- [106] G. Ramalho and K. Tsushima, Phys. Rev. D **84**, 054014 (2011) [arXiv:1107.1791 [hep-ph]].
- [107] G. Ramalho, K. Tsushima and F. Gross, Phys. Rev. D **80**, 033004 (2009) [arXiv:0907.1060 [hep-ph]].
- [108] G. Ramalho and M. T. Peña, Phys. Rev. D **83**, 054011 (2011) [arXiv:1012.2168 [hep-ph]].
- [109] G. Ramalho, K. Tsushima and A. W. Thomas, J. Phys. G **40**, 015102 (2013) [arXiv:1206.2207 [hep-ph]].
- [110] G. Ramalho and K. Tsushima, Phys. Rev. D **88**, 053002 (2013); [arXiv:1307.6840 [hep-ph]]. G. Ramalho and K. Tsushima, Phys. Rev. D **87**, 093011 (2013) [arXiv:1302.6889 [hep-ph]].
- [111] F. Gross, G. Ramalho and K. Tsushima, Phys. Lett. B **690**, 183 (2010) [arXiv:0910.2171 [hep-ph]].
- [112] G. Ramalho and K. Tsushima, Phys. Rev. D **86**, 114030 (2012) [arXiv:1210.7465 [hep-ph]].
- [113] G. Ramalho, M. T. Peña and A. Stadler, Phys. Rev. D **86**, 093022 (2012) [arXiv:1207.4392 [nucl-th]]; G. Ramalho and M. T. Peña, Phys. Rev. D **85**, 113014 (2012) [arXiv:1205.2575 [hep-ph]]; G. Ramalho, M. T. Peña, J. Weil, H. van Hees and U. Mosel, Phys. Rev. D **93**, 033004 (2016) [arXiv:1512.03764 [hep-ph]]; G. Ramalho, M. T. Peña and F. Gross, Phys. Rev. D **81**, 113011 (2010) [arXiv:1002.4170 [hep-ph]].
- [114] G. Ramalho, D. Jido and K. Tsushima, Phys. Rev. D **85**, 093014 (2012) [arXiv:1202.2299 [hep-ph]]; G. Ramalho and K. Tsushima, Phys. Rev. D **82**, 073007 (2010) [arXiv:1008.3822 [hep-ph]]; G. Ramalho and K. Tsushima, Phys. Rev. D **84**, 051301 (2011) [arXiv:1105.2484 [hep-ph]].
- [115] W. Greiner and B. Muller, *Quantum Mechanics symmetries*, 2nd edition, Springer-Verlag, New York, Berlin, Heidelberg (1994).
- [116] S. Gasiorowicz, *Elementary Particle Physics* John Wiley & Sons, Inc. New York, London, Sydney (1966).
- [117] D. B. Lichtenberg and L. J. Tassie, Phys. Rev. **155**, 1601 (1967).
- [118] E. Santopinto, Phys. Rev. C **72**, 022201 (2005) [hep-ph/0412319].
- [119] E. Santopinto and J. Ferretti, Phys. Rev. C **92**, no. 2, 025202 (2015) [arXiv:1412.7571 [nucl-th]].
- [120] M. L. Goldberger and S. B. Treiman, Phys. Rev. **110**, 1178 (1958).
- [121] S. Weinberg, Phys. Rev. Lett. **65**, 1181 (1990).
- [122] D. B. Leinweber, A. W. Thomas, K. Tsushima and S. V. Wright, Phys. Rev. D **64**, 094502 (2001) [arXiv:hep-lat/0104013].
- [123] C. Hayne and N. Isgur, Phys. Rev. D **25**, 1944 (1982).
- [124] I. Bender, V. Linke and H. J. Rothe, Z. Phys. **212**, 190 (1968).
- [125] V. Linke, Nucl. Phys. B **12**, 669 (1969).
- [126] C. E. Carlson and J. L. Poor, Phys. Rev. D **34**, 1478 (1986); C. E. Carlson and J. L. Poor, Phys. Rev. D **38**, 2758 (1988); C. E. Carlson and N. C. Mukhopadhyay, Phys. Rev. Lett. **81**, 2646 (1998) [hep-ph/9804356].